



EnMAP Ground Segment

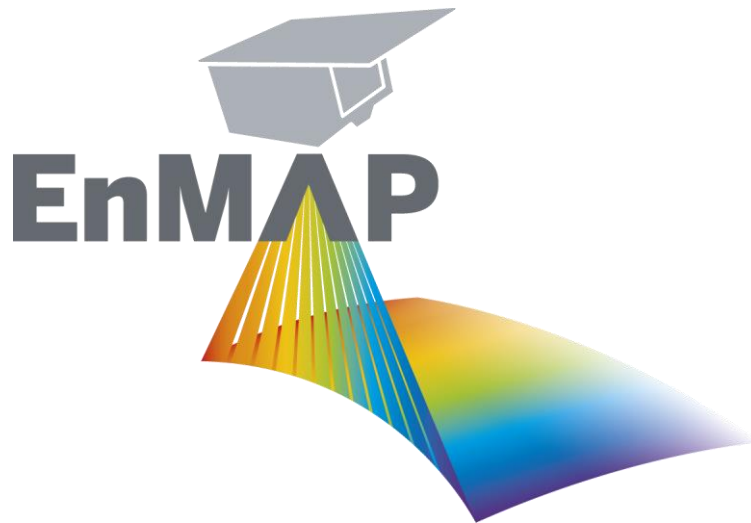
Mission Quarterly Report #06

01.10.2023 to 31.12.2023

Restriction: public

Doc. ID	EN-GS-RPT-1106
Issue	1.0
Date	21.02.2024

Configuration Controlled: Yes



German Remote Sensing Data Center (DFD)
Remote Sensing Technology Institute (IMF)
German Space Operations Center (GSOC)
German Research Centre for Geosciences (GFZ-Potsdam)
German Space Agency at DLR

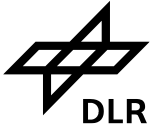


TABLE OF SIGNATURES

Prepared

Date Emiliano Carmona, (DLR MF-PBA, EnMAP OMM)

Date Sabine Chabrilat, (GFZ-Potsdam, EnMAP SciLead)

Reviewed

Date Katrin Wirth, (DLR RB-MIB, dep. EnMAP OMM)

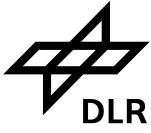
Date Sabine Engelbrecht, (DLR DFD-INF, EOC PAD)

Date Robert Größel, (DLR RB-CTA, GSOC PAD)

Date Karl Segl, (GFZ-Potsdam, dep. EnMAP SciLead)

Approved & Released

Date Sebastian Fischer, (DLR AR-AO, EnMAP MM)



DISTRIBUTION LIST

The document is publicly available via www.enmap.org.

CHANGE RECORD

Version	Date	Chapter	Comment
1.0	21.02.2023	All	First issue of Mission Quarterly Report #06

Custodian of this document is Carmona, Emiliano.



CONTENTS

Table of Signatures	2
Distribution List	3
Change Record	3
Contents	4
List of Figures	5
List of Tables.....	6
1 Introduction.....	8
1.1 Purpose	8
1.2 Scope	8
2 References	9
3 Terms, Definitions and Abbreviations	9
4 Mission	10
4.1 Mission Objectives	10
4.2 Mission Description	10
4.3 Mission Status Summary	11
5 Users and Announcements-of-Opportunities	13
5.1 Users	13
5.2 Announcements-of-Opportunities	14
6 Archived and Delivered Observations	16
6.1 Archived Observations	16
6.2 Delivered Observations.....	19
7 Detailed Status.....	21
7.1 User Interfaces.....	21
7.2 Satellite.....	21
7.2.1 Orbit	21
7.2.2 Life Limited Items.....	22
7.2.3 Redundancies	22
7.3 Ground Stations	23
7.3.1 S-Band	23
7.3.2 X-Band	23
7.4 Processors	23
7.5 Calibrations	24
7.5.1 Dead Pixels.....	26
7.5.2 Spectral Calibration	26
7.5.3 Radiometric Calibration	29
7.5.4 Geometric Calibration	36
7.6 Internal Quality Control	36
7.6.1 Archive.....	36
7.6.2 Level 1B.....	38
7.6.3 Level 1C.....	45
7.6.4 Level 2A.....	50
8 External Product Validation	60
8.1.1 Level 1B.....	60
8.1.2 Level 1C.....	60
8.1.3 Level 2A	61
8.1.4 Summary of External Product Monitoring.....	61
9 Others	62

LIST OF FIGURES

Figure 5-1	Number of registered users per country	14
Figure 6-1	Geographic location of all Earth observation tiles archived, World	17
Figure 6-2	Geographic location of all Earth observation tiles archived, Europe	18
Figure 6-3	Cloud coverage in [%] of archived Earth observation tiles	19
Figure 6-4	Observation angle of archived Earth observation tiles	19
Figure 6-5	Levels of delivered Earth observation tiles from acquisition orders	20
Figure 6-6	Levels of delivered Earth observation tiles from catalog orders	20
Figure 7-1	Number of ACS Precise Modes per day during 2023 Q4.....	22
Figure 7-2	Decay per day from Lamp (RAD), Linearity (LIN) and Spectral (SPC) measurements for low gain (top) and high gain (bottom)	25
Figure 7-3	Average percentage change in the VNIR radiometric coefficients for five selected bands since launch.....	25
Figure 7-4	VNIR Dead Pixel Mask	26
Figure 7-5	SWIR Dead Pixel Mask.....	26
Figure 7-6	VNIR (top) and SWIR (bottom) center wavelength in nm.....	28
Figure 7-7	Change in center wavelength per spectral pixel for VNIR (top) and SWIR (bottom).....	28
Figure 7-8	VNIR (top) and SWIR (bottom) FWHM in nm	29
Figure 7-9	VNIR (top) and SWIR (bottom) calibration coefficient in mW/cm ² /sr/μm.....	31
Figure 7-10	Percentage change in VNIR Calibration Coefficients (top) and SWIR Calibration Coefficients (bottom).....	32
Figure 7-11	VNIR (top) and SWIR (bottom) gain matching calibration coefficients	32
Figure 7-12	VNIR (top) and SWIR (bottom) response non-uniformity coefficients	33
Figure 7-13	SNR contour map for VNIR high gain from the LED linearity observations observed on 08.11.2023. The solar reference spectrum is shown with a blue line. Contour lines with SNR values of 150 and 500 are also shown in black.	34
Figure 7-14	SNR contour map for VNIR low gain from the LED linearity observations observed on 08.11.2023. The solar reference spectrum is shown with a blue line and the position of the requirement is marked on the reference spectrum with a black cross. Contour lines with SNR values of 150 and 500 are also shown in black.	34
Figure 7-15	SNR contour map for SWIR high gain from the LED linearity observations observed on 08.11.2023. The solar reference spectrum is shown with a blue line and the position of the requirement is marked on the reference spectrum with a black cross. Contour lines with SNR values of 150 and 500 are also shown in black.	35
Figure 7-16	SNR contour map for SWIR low gain from the LED linearity observations observed on 08.11.2023. The solar reference spectrum is shown with a blue line. Contour lines with SNR values of 150 and 500 are also shown in black.	35
Figure 7-17	VNIR estimated spectral shift at 760 nm w.r.t the nominal band center, and relative spectral stability expressed at 1 sigma (Q3 2023).....	41
Figure 7-18	SWIR estimated spectral shift at 2050 nm w.r.t the nominal band center, and relative spectral stability expressed at 1 sigma (Q3 2023).....	41
Figure 7-19	Center wavelengths per cross-track pixel based on the spectral calibration table (VNIR band 62).....	42
Figure 7-20	VNIR estimated spectral shift at 760 nm w.r.t the valid spectral calibration table (CTB_SPC), and relative spectral stability expressed at 1 sigma (Q4 2023, 7419 tiles)	42
Figure 7-21	Center wavelengths per cross-track pixel based on the spectral calibration table (SWIR band 86).....	43

Figure 7-22 SWIR estimated spectral shift at 2050 nm w.r.t the valid spectral calibration table (CTB_SPC), and relative spectral stability expressed at 1 sigma (Q4 2023, 7419 tiles)	43
Figure 7-23 Datatake used (North Australia).....	44
Figure 7-24 Datatake used (US Westcoast).....	44
Figure 7-25 Datatake used (Memphis, USA)	45
Figure 7-26 Assessment of RMSE values, calculated based on found ICPs, for all datatakes where ICP could be found	46
Figure 7-27 Mean deviation of EnMAP L1C products in pixel (left). RMSE value for EnMAP L1C products in pixel (right).....	47
Figure 7-28 Mean deviation in pixel between VNIR and SWIR data of EnMAP L1C products (left). RMSE in pixel between VNIR and SWIR data of EnMAP L1C Products (right).....	48
Figure 7-29 Development of co-registration accuracy based on the previous geometric QC reports ..	49
Figure 7-30 RGB - Quicklook of sceneID 48673; Red frame is the AOI for further investigation, the crosses show the sample – locations for the following analysis; Wavelengths for RGB: 611.02nm – 550.69nm – 463.73nm	51
Figure 7-31 Masking within the AOI; Land in green, clouds in brown, water in blue	51
Figure 7-32 Red is the radiance without adjacency correction, blue corresponds to the spectrum after correction; Left: AC 1, Right: AC 2.....	52
Figure 7-33 Quality mask for the AOI in greyscale of total quality	52
Figure 7-34 Water Leaving Reflectance for the AOI; Wavelengths for RGB: 611.02nm – 550.69nm – 463.73nm	53
Figure 7-35 Water leaving reflectance for locations ‘Reflectance 1’ on the left and ‘Reflectance 2’ on the right	53
Figure 7-36 From left to right: EnMAP L2A CIR, quality classes, Google Earth	55
Figure 7-37 Left: EnMAP L2A, Right: QL classes (blue = water, green = land).....	56
Figure 7-38 From left to right: EnMAP L2A RGB, quality classes (red = cloud)	56
Figure 7-39 Left: EnMAP L2A, : Middle: QL classes (blue = water, green = land); Right: EnMAP L2A overlaid by haze mask	57
Figure 7-40 From Left: EnMAP L2A (CIR); QL classes (blue = water, green = land); EnMAP L2A (RGB) overlaid by haze mask; Haze mask	57
Figure 7-41 From Left: EnMAP L2A (CIR); QL classes (blue = water, green = land); EnMAP L2A (RGB), image stretched; Haze mask	58
Figure 7-42 Reflectance of smoke plume displaying the position of the corresponding pixel in the scene (EnMAP L2A and QL classes)	58
Figure 7-43 From Left: EnMAP L2A (CIR); QL classes (blue = water, green = land); Snow mask, Google Earth.....	59
Figure 7-44 Spectra collected within the areas classified as snow (colored) and outside (black)	59

LIST OF TABLES

Table 2-1	References.....	9
Table 5-1	Number of registered users per continent (number of user countries during reporting period)	13
Table 5-2	Number of registered users per category (Cat-1 Science and Cat-1 Distributor).....	14
Table 5-3	Number of released science proposals per Announcement-of-Opportunity (AOs#) and total number of requested and granted tiles per AO#.....	14

Table 5-4	Number of accepted science proposals and total number of requested and granted tiles per topic	15
Table 6-1	Number and size of archived and not archived products	16
Table 6-2	Number and size of delivered products	16
Table 7-1	Status of life-limited items. Items marked with (*) obtained from estimation pending finalization of the calculations.	22
Table 7-2	S-Band Ground Station Passes	23
Table 7-3	X-Band Ground Station Passes	23
Table 7-4	Number and size of archived radiometric and spectral calibration observations	24
Table 7-5	Number and percent of dead pixels	26
Table 7-6	Number and size of archived spectral calibration observations	26
Table 7-7	Generated spectral calibration tables	29
Table 7-8	Number and size of archived radiometric calibration observations	30
Table 7-9	Generated radiometric calibration tables	36
Table 7-10	Generated new geometric calibration tables	36
Table 7-11	Overall quality rating statistics	37
Table 7-12	Overall quality rating in relation to Sun Zenith Angle (SZA)	37
Table 7-13	Reduced and low quality rating statistics	37
Table 7-14	QualityAtmosphere rating statistics	37
Table 7-15	QualityAtmosphere rating in relation to Sun Zenith Angle (SZA)	38
Table 7-16	QualityAtmosphere rating in relation to Cloud Cover and DDV availability	38
Table 7-17	Dead pixel statistics, VNIR	39
Table 7-18	Dead pixel statistics, SWIR	39
Table 7-19	Saturation statistics, VNIR	40
Table 7-20	Saturation statistics, SWIR	40
Table 7-21	Artifacts statistics (without striping), VNIR	40
Table 7-22	Artifact statistics (without striping), SWIR	40
Table 7-23	Validated CTB_RAD	43
Table 7-24	Validated CTB_SPC	45
Table 7-25	Improvement of geometric performance	48
Table 7-26	Datatake ID of analyzed land products	54



1 Introduction

1.1 Purpose

This mission quarterly report (MQR) states information on the EnMAP mission status with regard to the registered user community, announcements-of-opportunities and observations as well as the status of the user interfaces, satellite (platform and payload), ground stations (S-band and X-band), processor (Archive, Level 1B, Level 1C, Level 2A (land and water)), calibration (spectral, radiometric, geometric), data quality control and validation of EnMAP.

Please visit www.enmap.org for further information on EnMAP.

1.2 Scope

This sixth Mission Quarterly Report (MQR) applies to the operations of EnMAP in the reporting period of Routine Phase (RP) from **01.10.2023** to **31.12.2023 (Q4/2023)**.

2 References

Reference Identifier	Document Identifier and Title
[1]	L. Guanter et al. (2015) The EnMAP Spaceborne Imaging Spectroscopy Mission for Earth Observation. Remote Sensing, Issue 7, pp. 8830-8857.
[2]	EN-GS-UM-6020 Portals User Manual, Version 1.4
[3]	EN-PCV-ICD-2009 Product Specification, Version 1.8
[4]	EN-PCV-TN-4006 Level 1B ATBD, Version 1.7
[5]	EN-PCV-TN-5006 Level 1C ATBD, Version 1.6
[6]	EN-PCV-TN-6007 Level 2A (land) ATBD, Version 2.2
[7]	EN-PCV-TN-6008 Level 2A (water) ATBD, Version 3.1
[8]	Chabrillat, S. et al. (2022) EnMAP Science Plan. EnMAP Technical Report, DOI: 10.48440/enmap.2022.001
[9]	Storch, T.; Honold, H.-P.; Chabrillat, et al. The EnMAP imaging spectroscopy mission towards operations. Remote Sens. Environ. 2023, 294, 113632. DOI: 10.1016/j.rse.2023.113632

Table 2-1 References

3 Terms, Definitions and Abbreviations

Terms, definitions and abbreviations for EnMAP are collected in a database which is publicly accessible via Internet on www.enmap.org.

An Earth observation of swath length $n \times 30$ km (and swath width 30 km) is separated into n tiles of size 30 km \times 30 km.

4 Mission

4.1 Mission Objectives

The primary goal of EnMAP (Environmental Mapping and Analysis Program) is to measure, derive and analyze quantitative diagnostic parameters describing key processes on the Earth's surface [1].

During the mission operations, with the successful launch on 1st of April 2022 and an expected operational mission lifetime of at least 5 years, EnMAP will provide valuable information for various application fields comprising soil and geology, agriculture, forestry, urban areas, aquatic systems, ecosystem transitions.

4.2 Mission Description

The major elements of the EnMAP mission are the EnMAP Space Segment, built by OHB System AG and owned by the German Space Agency at DLR, the EnMAP Ground Segment built and operated by DLR institutes DFD, MF, RB, and the EnMAP User and Science Segment represented by GFZ. The project management of the EnMAP mission is responsibility of the German Space Agency at DLR.

The EnMAP Space Segment is composed of

- the platform providing power and thermal stability, orbit and attitude control, memory, S-band uplink/downlink for TM/TC data transmission/reception, X-band downlink for payload data transmission, and
- the payload realized as a pushbroom imaging dual-spectrometer covering the wavelength range between 420 nm and 2450 nm with a nominal spectral resolution ≤ 10 nm and allows in combination with a high radiometric resolution and stability to measure subtle reflectance changes.

The EnMAP satellite is operated on a sun-synchronous repeat orbit to observe any location on the globe with comparable illumination conditions. This allows a maximum reflected solar input radiance at the sensor with an acceptable risk for cloud coverage.

The EnMAP Ground Segment is the interface between Space Segment and User and Science Segment. It comprises functionalities to

- perform planning of imaging, communication and orbit maneuver operations, provision of orbit and attitude data, command and control of the satellite, ground station networks (in particular: Weilheim, Germany, for S-band and Neustrelitz, Germany, for X-Band), receive satellite data, perform long-term archiving and delivery of products, and
- perform processing chain (for systematic and radiometric correction, orthorectification, atmospheric compensation), instrument calibration operations, and the data quality control of the products.

The EnMAP mission interfaces to the international science and user community through the EnMAP Portal www.enmap.org with official information related to EnMAP by DLR and GFZ-Potsdam (as the document in hand) and links for ordering observations and products.

The EnMAP Science Segment is represented by the EnMAP Science Advisory Group chaired by the mission principal investigator at the GFZ-Potsdam. The Science Segment addresses aspects such as

- supporting and performing validation activities to improve sensor performance and product quality
- developing scientific and application research to fully exploit the scientific potential of EnMAP [8] including provision of software tools for EnMAP data processing and analyses (EnMAP-Box) and provision of teaching and education materials (HYPERedu)
- Organizing workshops, summer schools and in general information, training and networking activities for the user community

The EnMAP User Segment is the community of German and international users ordering acquisitions and accessing products of EnMAP.

4.3 Mission Status Summary

The mission successfully finished the commissioning phase (CP) on 01.11.2022 [9] and entered its routine phase (RP) on 02.11.2022. In the reporting period between 01.10.2023 and 31.12.2023 there have been no major issues affecting the instrument or the satellite. There has been, though, two outages (13.10.2023 – 27.10.2023 and 07.12.2023 – 19.12.2023) caused by the same root cause (a jump in time that confused the thermal control system of the satellite, causing a controlled shutdown) that resulted in the loss of observation time (no other known consequences with current knowledge). New occurrences of these events are not expected after the software update performed in January 2024. An occurrence of the DSHA safety mode also caused the loss of observations from 24.11.2023 to 26.11.2023. By the end of 2023, the EnMAP mission is regularly reaching the maximum acquisition capacity of 5000 km / day.

In this period, 968 Earth observations of 30 km swath width and up to 990 km swath length were successfully performed which resulted in 7372 archived Earth observation tiles of 30 km x 30 km and 21 calibration acquisitions. In total, 7654 Earth observations were performed until 31.12.2023 by the EnMAP team and the 1746 registered Science users which resulted in 47816 archived Earth observation tiles (58469 including re-processed products) and 44904 Earth observation tiles delivered to users since the start of the mission. More details are presented in Section 5 and 6.

The following limitations are applicable at 31.12.2023:

- Some striping effects in SWIR data in the along-track direction more visible in uniform areas with a strong spectral gradient.
- In L2A-water processing, the glint – band within the quality-mask is set to 1, even if there is actual sun-glint present. It is suggested that the users don't use the mentioned band until the corresponding bug is fixed.
- Water turbidity option in L2A-water processing is not correctly handled and all scenes are processed as "clear water".

Other effects observed in the data by our Quality Control team are reported in section 7.6 while they are investigated in more detail.

The following changes were implemented in the reporting period:

- After middle of October, the mission returned to fully automatic processing of acquisition requests by the Mission Planning System. When the total number of requests was below the limit and request queue fully processed, the system could be returned to its default functioning mode (automatic processing).
- Full integration of Inuvik station for additional X-Band data reception after successful completion of X-Band tests.
- It has been fixed the issue that caused a difference between the coordinates entered in the planning tool and the coordinates acquired. As a consequence of this issue, in some occasions (1 tile observations at large off-nadir angles) the planning coordinate could even be outside the acquired product. By the end of December 2023, an update of the mission planning software was performed solving this issue. The checks performed by the GS team after the update show that the maximum error to be expected in the future is always under 3.5 km (in accordance with the expected accuracy of the platform).
- SNR calculation is updated after removing filtering of frames that artificially reduced the noise estimation.
- Fixed a problem that produced peaks in L2A-land spectra over snow.
- Re-processing of archived products is in progress. Priority processing is now assigned to the oldest data (commissioning phase). On these data the co-registration errors are larger, what makes the re-processing of the data more necessary for them. Reprocessed products can be identified with **archived version \geq 01.03.01** in the EnMAP archive. Re-processed products benefit from improved co-registration accuracy, improved absolute geometric performance and addition of VC-AUX products for improved data screening. The re-processing will continue over the coming months. For more details on geometric performance check Section 7.6.3.

The following changes are expected to be performed in the next quarters:

- Correction of radiometric striping in the along-track direction.
- Continue re-processing of archived data (see note above concerning re-processed data improvements).
- New version of the MIP program for L2A-water processing will improve/solve the following aspects:
 - Reduce spectral peaks in the reflectance spectra around Fraunhofer lines
 - Water turbidity option correctly interpreted
 - Issue with glint-band values
- Implementation of back-to-back imaging what shall reduce in certain circumstances the minimum distance between consecutive acquisitions
- Implementation of new measures to improve planning and acquisition activities

5 Users and Announcements-of-Opportunities

5.1 Users

	Country/Continent (No of Countries)	Reporting Period 01.10.2023 to 31.12.2023	Since beginning of routine Phase until 31.12.2023 (end of reporting period)
<i>Total European Users</i>	<i>Europe (21)</i>	183	1222
European	• Germany	61	533
	• Italy	16	116
	• France	22	88
	• Great Britain	14	74
	• Spain	11	51
	• Netherlands	6	45
	• Portugal	3	23
	• Turkey	8	40
	• Greece	6	26
	• Belgium	3	23
	• Poland	7	31
	• Austria	2	17
	• Others (10)	24	155
<i>Non European</i>	<i>North America (2)</i>	57	298
	<i>South America (6)</i>	31	152
	<i>Asia (17)</i>	129	457
	<i>Africa (9)</i>	24	124
	<i>Australia + New Zealand (2)</i>	17	95
	<i>Total (58)</i>	441	2356
	<i>Rejected*</i>	2	7

Table 5-1 Number of registered users per continent (**number of user countries during reporting period**)

*Users are rejected because of, e.g. EU sanction list checks, data policy or license violations.

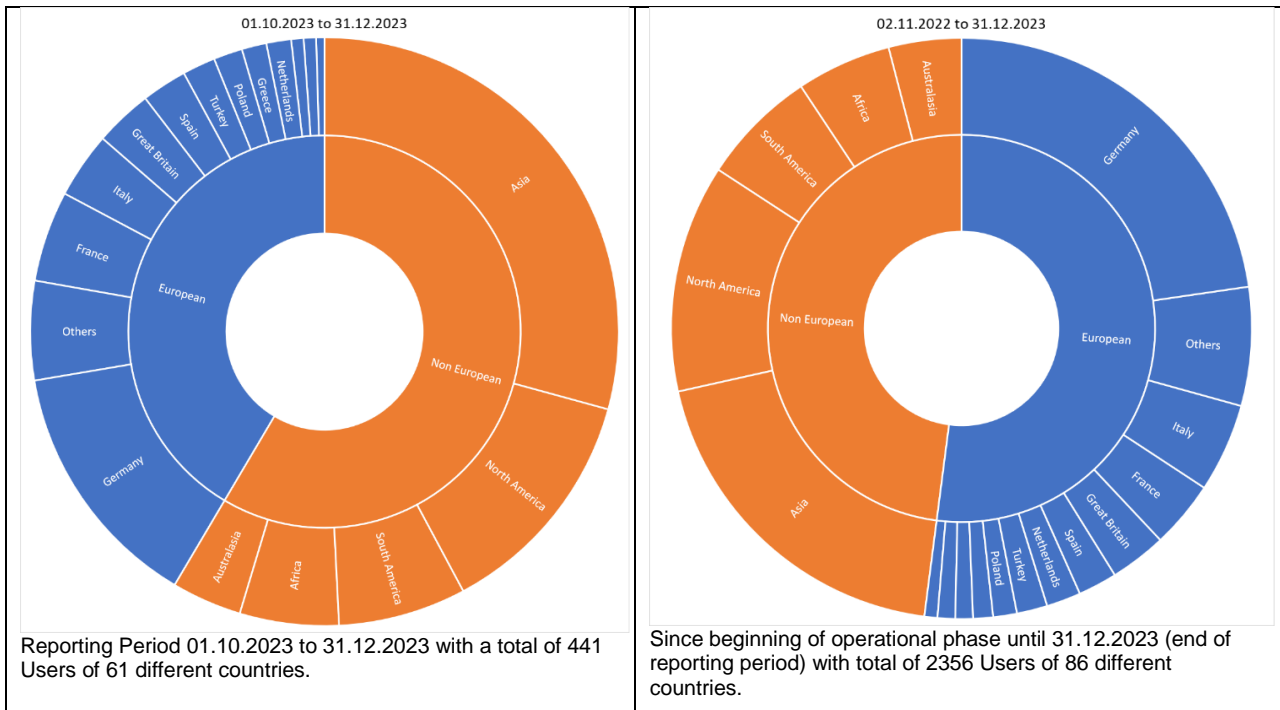


Figure 5-1 Number of registered users per country

Registered users belong to different categories, therefore e.g. All/World \neq Science/World + Others/World.

User per Category		Reporting Period 01.10.2023 to 31.12.2023	Since beginning of routine phase start until 31.12.2023 (end of reporting period)
Registered users	Total	441	2356
	with role assignment*	347	1746
Cat-1 Science	Total	275	1372
	AO Process 00001	275	1267
	AO Process 00002	0	615
	AO Process 00003	0	194
Cat-1 Distributor**	Total	292	1301

Table 5-2 Number of registered users per category (Cat-1 Science and Cat-1 Distributor)

*Registered users with at least one user role assignment

**Catalogue User, ordering EnMAP data from archive

5.2 Announcements-of-Opportunities

Announcement-of-Opportunity	Reporting Period 01.10.2023 to 31.12.2023			Since beginning of routine Phase until 31.12.2023 (end of reporting period)		
	Proposals	Total tiles requested	Total tiles granted	Proposals	Total tiles requested	Total tiles granted
A00001	57	4877	1329	304	21106	12357
A00002	4	1416	573	123	20430	9339
A00003	0	0	0	4	151	97
Total	61	6293	1902	431	41687	21793

Table 5-3 Number of released science proposals per Announcement-of-Opportunity (AOs#) and total number of requested and granted tiles per AO#.










Icon	Topic	Reporting Period 01.10.2023 to 31.12.2023			Since beginning of routine Phase until 31.12.2023 (end of reporting period)		
		Proposal	Total tiles requested	Total tiles granted	Proposal	Total tiles requested	Total tiles granted
	VEGETATION	19	3690	785	170	22688	10286
	GEO/SOIL	28	1616	785	136	5699	3717
	WATER	7	568	198	52	3024	2546
	SNOW/ICE	0	0	0	7	1856	698
	URBAN	0	0	0	8	774	307
	ATMOSPHERE	4	366	123	14	2904	1170
	HAZARD/RISK	1	4	5	9	283	241
	METHODS	0	0	0	13	937	537
	CAL/VAL	0	0	0	22	3522	2291
	Total	61	6293	1902	431	41687	21793

Table 5-4 Number of accepted science proposals and total number of requested and granted tiles per topic

6 Archived and Delivered Observations

The following table shows the number of archived Earth Observation and Calibration products and their sizes within the specified time frames. Reason for “Archived = No” is that datatakes were commanded but no data arrived at the Processing System HSI.

Type	Archived		Reporting Period 01.10.2023 to 31.12.2023		Since beginning of Commissioning Phase until 31.12.2023 (end of reporting period)	
			Number Tiles / Observations	Size (in GB)	Number Tiles / Observations	Size (in GB)
Earth Observation (EO)	Yes	Total	7372 / 968	3592.13	58469 / 7654	28490.07
		Average / Day	80.13 / 10.52	39.04	91.35 / 11.95	44.51
	No	Total	24		863	
		Average / Day	0.26		1.34	
Calibration (CAL)	Yes	Total	21	87.69	198	826.79
		Average / Day	0.22	0.95	0.30	1.29
	No	Total	1		2	
		Average / Day	0.01		0.003	

Table 6-1 Number and size of archived and not archived products

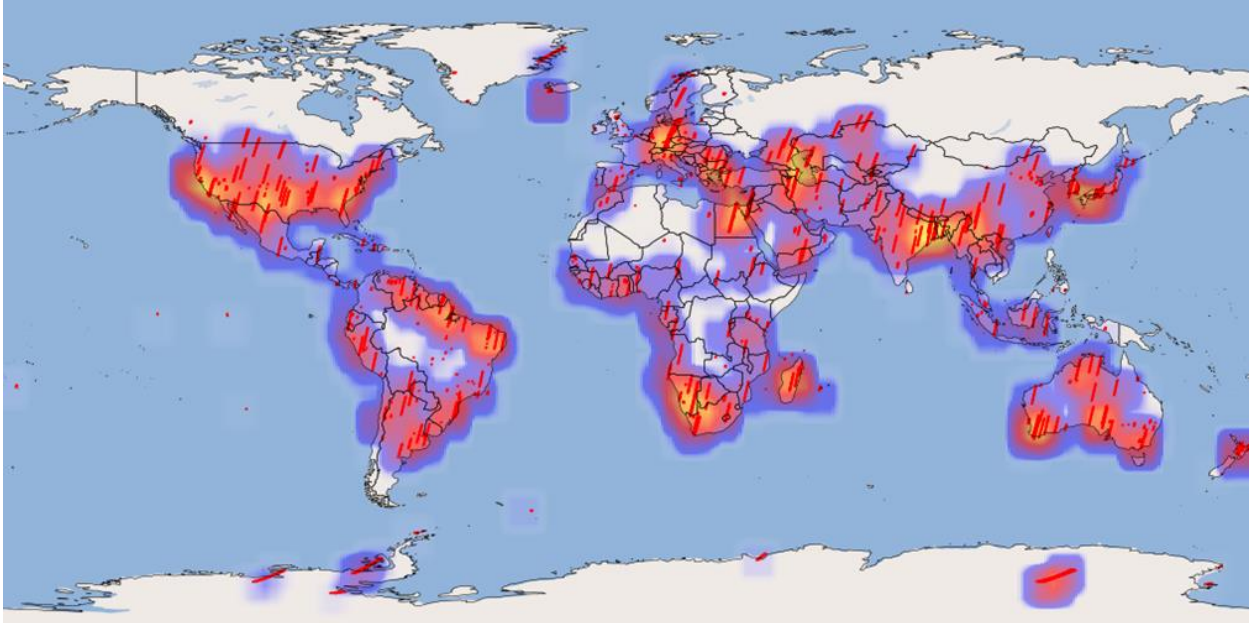
The following table shows the number of delivered products and their sizes within the specified time frames. Product deliveries result either directly from acquisition orders (“Observation”) or catalog orders (“Archive”).

Type	Delivered		Reporting Period 01.10.2023 to 31.12.2023		Since beginning of Commissioning Phase until 31.12.2023 (end of reporting period)	
			Number Tiles / Observations	Size (in GB)	Number Tiles / Observations	Size (in GB)
Earth Observation (EO)	Observation	Total	7442 / 757	3229.83	44904 / 5565 ⁽¹⁾	19304 ⁽¹⁾
		Average / Day	80.89 / 8.22	35.10	70.16 / 8.69	30.16 ⁽¹⁾
	Archive	Total	8114	43822.83	33134	178362.30
		Average / Day	88.19	476.33	51.77	278.69
Calibration (CAL)	Observation	Total	22	82.33	123	541.40
		Average / Day	0.23	0.89	0.19	0.84
	Archive	Total	2	5.17	68	3486.92
		Average / Day	0.02	0.05	0.10	5.44

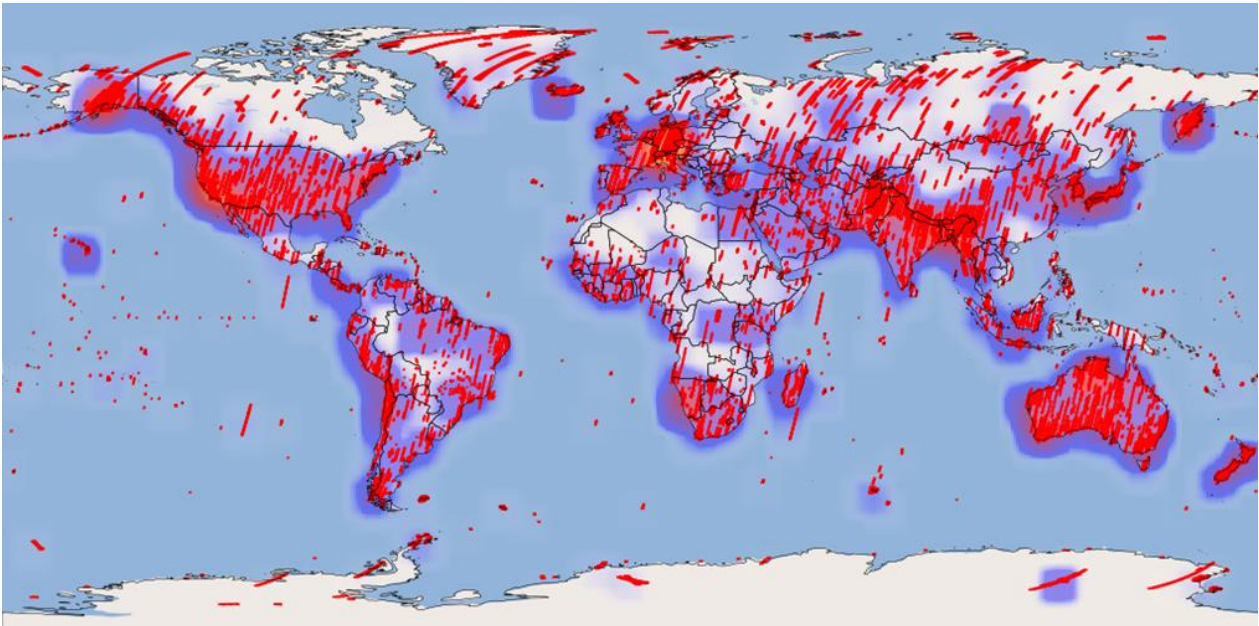
Table 6-2 Number and size of delivered products

6.1 Archived Observations

The following figures show the heatmaps for the whole world and for Europe within the specified time frames. The heatmaps represent the frequencies of products at a geographic location, where the number of products increases from blue over red to yellow.

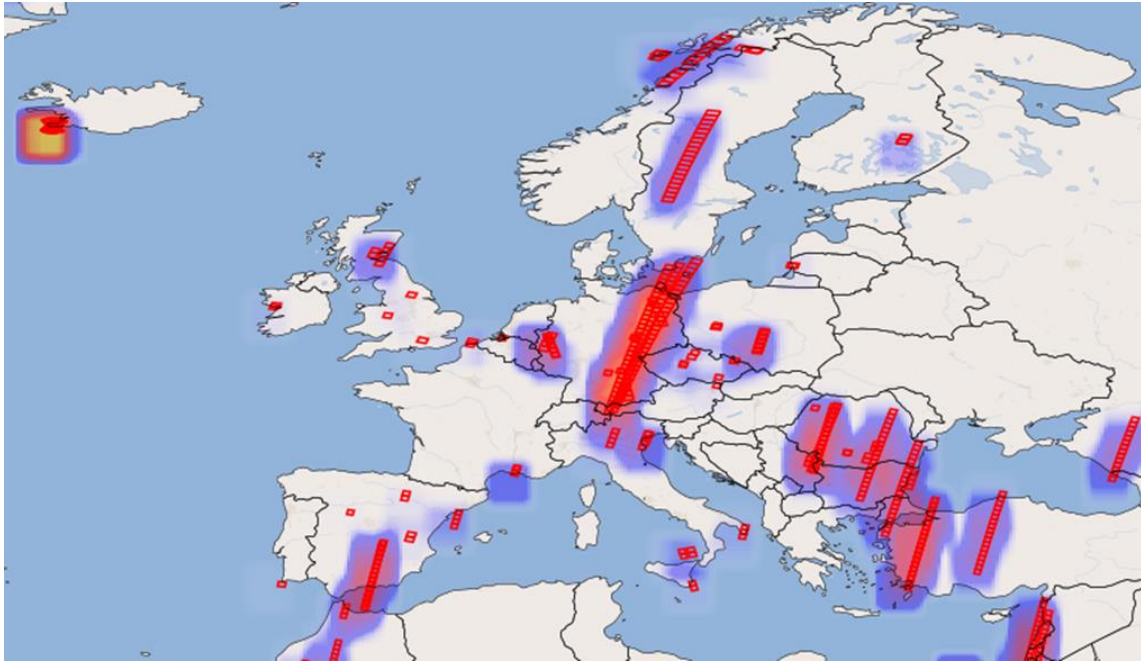


01.10.2023 to 31.12.2023 with 7372 tiles

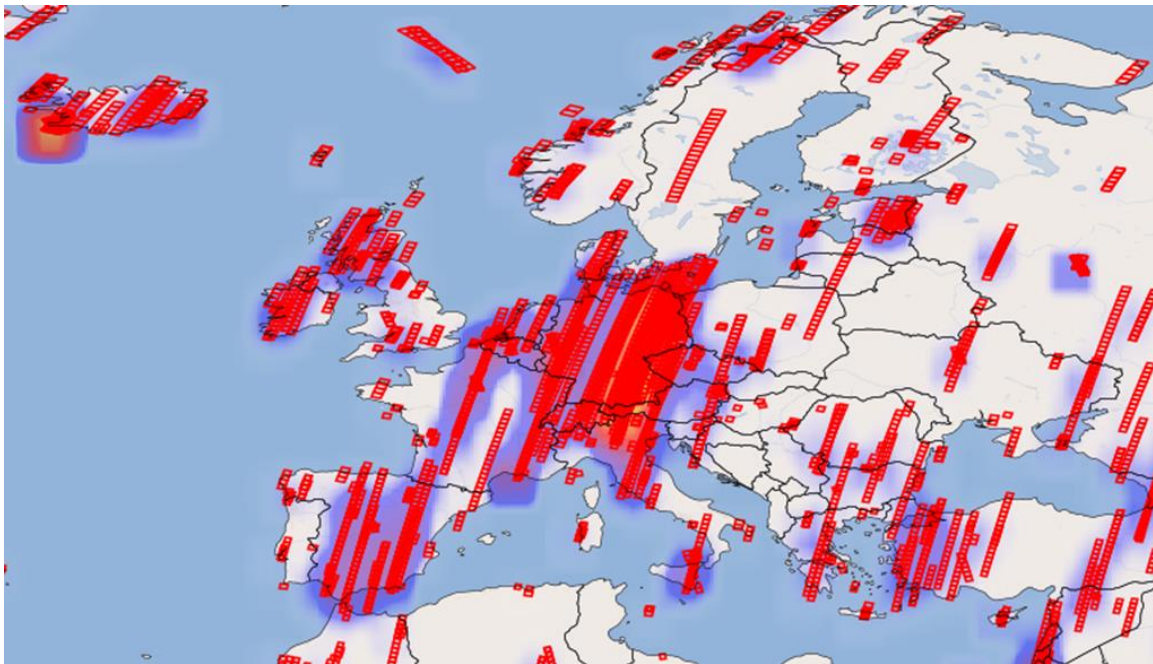


until 31.12.2023 with 58469 tiles (includes commissioning phase acquisitions)

Figure 6-1 Geographic location of all Earth observation tiles archived, World



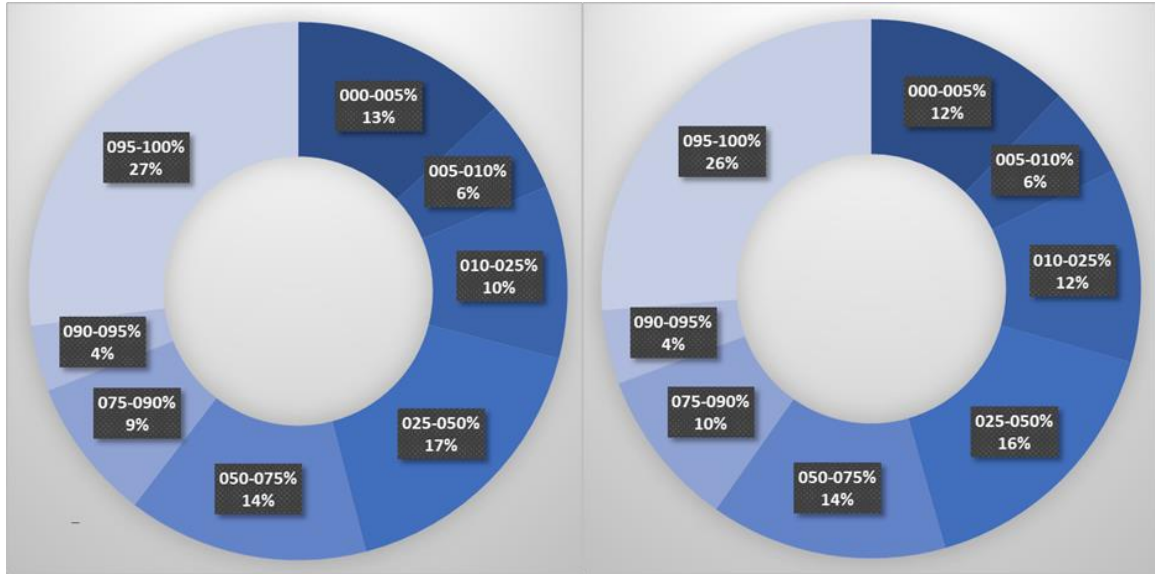
01.10.2023 to 31.12.2023



until 31.12.2023 (includes commissioning phase acquisitions)

Figure 6-2 Geographic location of all Earth observation tiles archived, Europe

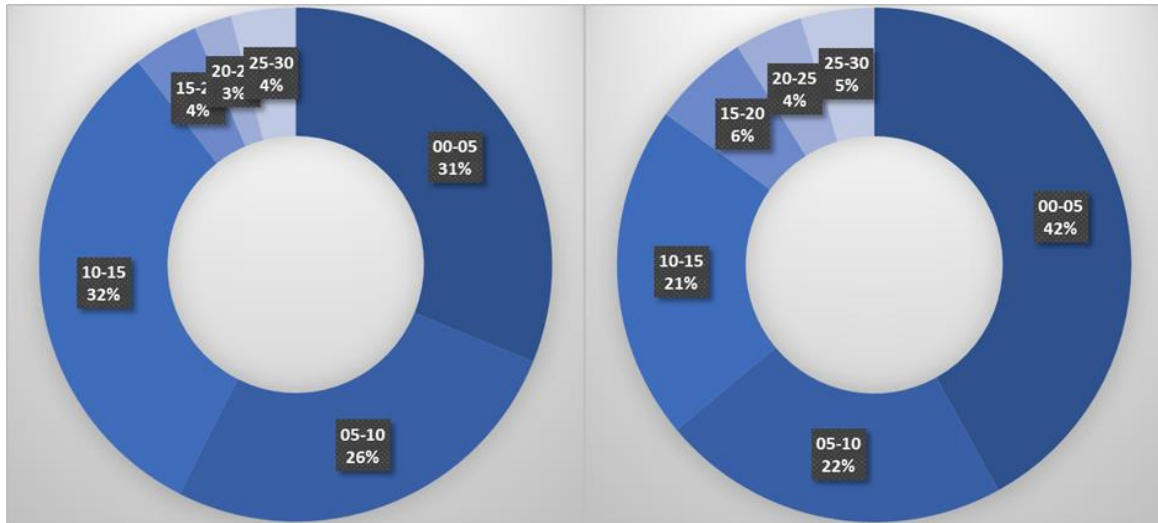
The following figures show the distribution of cloud coverage for the archived products.



01.10.2023 to 31.12.2023 with 7372 tiles until 31.12.2023 with 58548 tiles (includes commissioning)

Figure 6-3 Cloud coverage in [%] of archived Earth observation tiles

The following figures show the distribution of observation angles for the archived products.

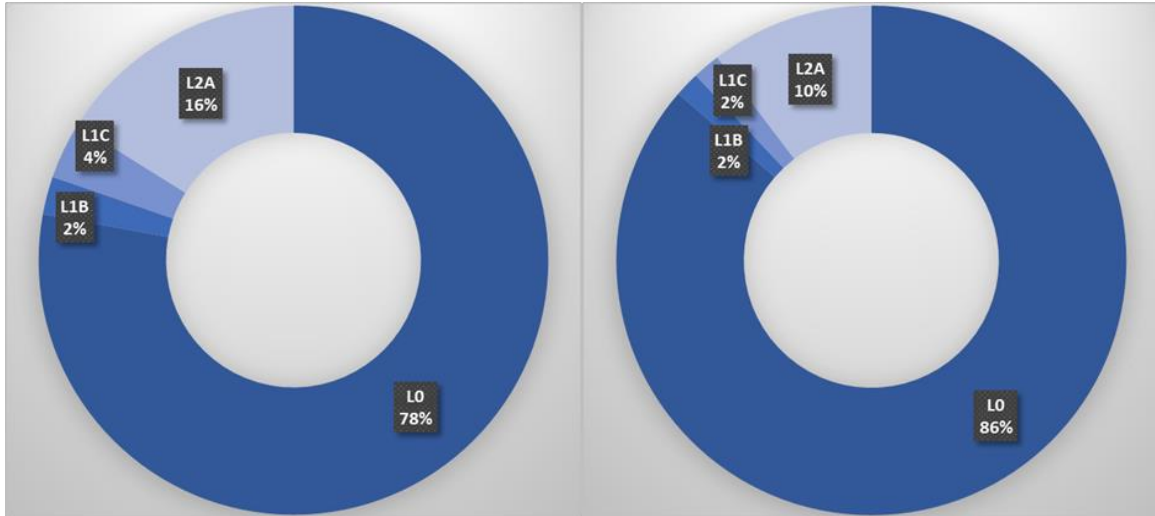


01.10.2023 to 31.12.2023 with 7372 tiles until 31.12.2023 with 58548 tiles (includes commissioning)

Figure 6-4 Observation angle of archived Earth observation tiles

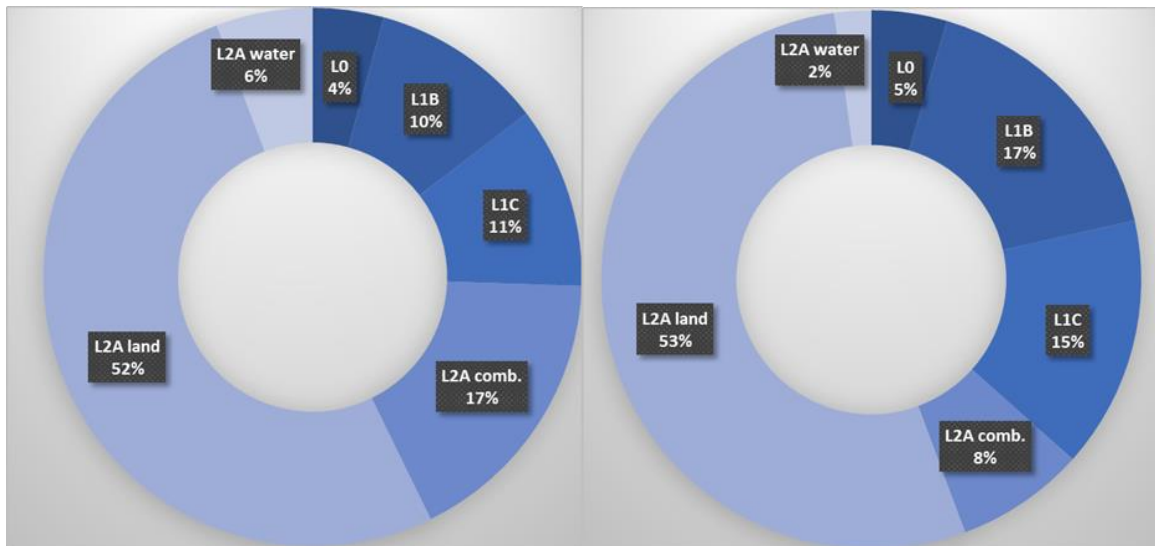
6.2 Delivered Observations

The following figures show the distribution of processing level of the delivered products from acquisition orders.



01.10.2023 to 31.12.2023 with 7442 tiles until 31.12.2023 with 47369 tiles (includes commissioning)
Figure 6-5 Levels of delivered Earth observation tiles from acquisition orders

The following figures show the distribution of processing level and correction type (for L2A) of the delivered products from catalog orders.



01.10.2023 to 31.12.2023 with 8114 tiles until 31.12.2023 with 28994 tiles (includes commissioning)
Figure 6-6 Levels of delivered Earth observation tiles from catalog orders

7 Detailed Status

7.1 User Interfaces

Further improvements to the user interfaces are continuously on-going and will be reported in this section.

7.2 Satellite

No major satellite issues have been observed in the reporting period. There have been, however, three outages that have caused loss of observation time (no other known consequences with current knowledge). The outages taken place between 13 October to 27 October and between 7 December and 19 December have the same origin. A jump back in time in the satellite timing system (root cause not known) triggered severe instabilities in the instrument thermal control system and forced an automated safety shutdown of the hyperspectral imager. Recovery time took several days in order to analyze the data and prepare a stepwise power up which is a time-consuming process. To prevent further occurrences of this issue, a software update has been prepared by the Space Segment and at the time of writing this report it was already installed on-board by the Ground Segment. The third outage in the reporting period took place between 24 and 26 November due to the well-known issue of the DSHA Safety Mode. In this case, no new observations could be stored during the weekend until the DSHA was reset.

On the ground systems, the number of acquisition requests was still over the system limit at the start of the reporting period. As expected, the number of requests was reducing over time and by the middle of October there were no more queued requests and the total number was below the system limit. At this point the system could be returned to the default configuration, the automatic forwarding of acquisition requests from the Instrument Planning System to the Mission Planning System. It shall be noticed that an increase on requests from the users can cause again an overflow of requests, unless other mitigation measures are implemented to prevent these situations in the future.

7.2.1 Orbit

The reference orbit is a Sun-synchronous polar orbit with a mean local time of descending node of 11:00 hrs and a repeat cycle of 398 revolutions in 27 days at an altitude of 643 km (lateral deviation of at most 22 km at equator and altitude deviation of at most 6 km).

During 2023 Q3, a total of two in-plane and one out-of-plane orbit maneuvers were executed. No collision avoidance maneuvers were required. The resulting performance error off all maneuvers was estimated by FDS to be between -0.5 % and +0.7 %. All executed orbit maneuvers of 2023 Q3 are listed in Table 4 1. Both OCS thrusters were actuated a total of three times during the above-mentioned orbit maneuvers. No actuations of the Ball Latch Valve or other OCS configuration changes were performed during 2023 Q3.

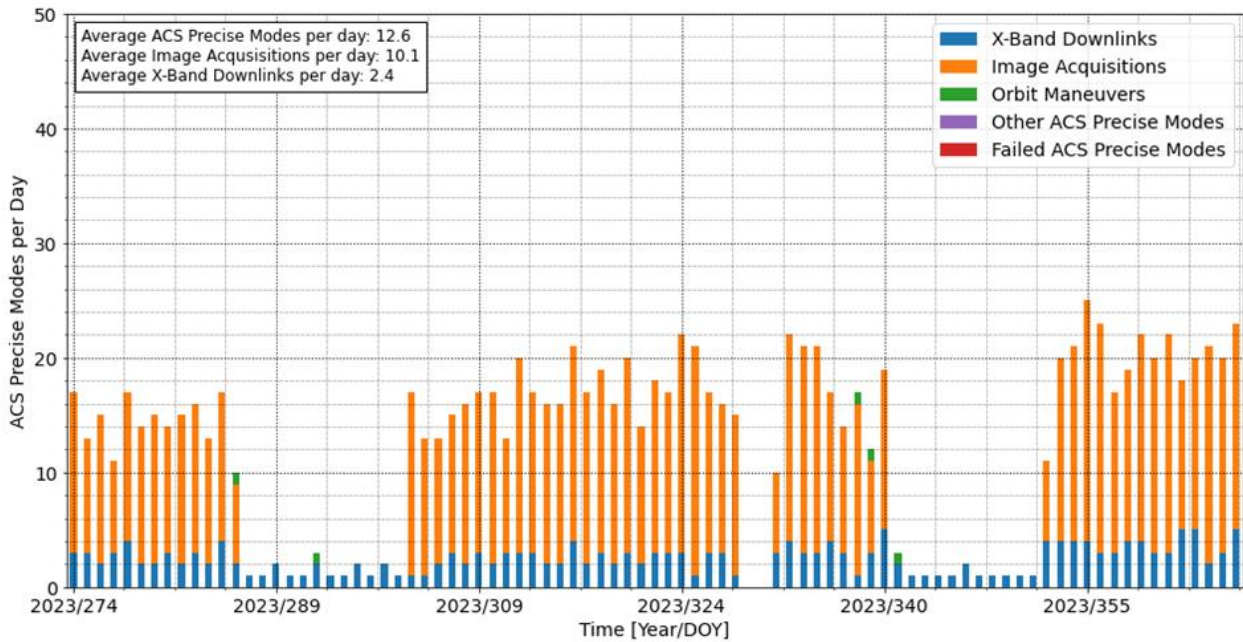


Figure 7-1 Number of ACS Precise Modes per day during 2023 Q4

7.2.2 Life Limited Items

Life-Limited Item	01.10.2023 to 31.12.2023	until 31.12.2023	Estimated total usage
Fuel	+0.6 kg	5.1 kg	>15 years
Battery and Solar Cells	nominal	nominal	nominal
Shutter Usage ^(*)	+1,12%	8,73%	20 years (@ daily use)
FAD movements ^(*)	+2,00%	18,00%	8,6 years (@ monthly use)
Diffuser exposure ^(*) time based on sole measurement time	+3,33%	30,00%	5,3 years (@ monthly use)
Diffuser exposure ^(*) time based on real cyclogram duration	+3,96%	35,63%	4,5 years (@ monthly use)
On-Board Calibration Equipment Usage ^(*)	On-board calibration equipment:		
- OBCA SPC lamp 1	+1,00%	8,03%	19,3 years (@ biweekly use)
- OBCA RAD lamp 1/LED 1	+2,61%	14,35%	8 years (@ weekly use)
- FPA LEDs 1	+0,37%	4,12%	44,4 years (@ monthly use)

Table 7-1 Status of life-limited items. Items marked with ^(*) obtained from estimation pending finalization of the calculations.

7.2.3 Redundancies

To date, the SWIR wavelength range is covered by SWIR-A (SWIR-B can be activated using a one-time switch mechanism).

All satellite subsystems are using nominal configurations.

7.3 Ground Stations

7.3.1 S-Band

S-Band Ground Stations	01.10.2023 to 31.12.2023		
	Total Passes	Non-Routine Passes (e.g. Anomaly Handling/SW Updates)	Failed Passes
All stations (Weilheim-Germany, Neustrelitz-Germany, Inuvik,-Canada, O'Higgins-Antarctica, Svalbard-Norway)	471 (70 INU)	38	6

Table 7-2 S-Band Ground Station Passes

7.3.2 X-Band

X-Band Ground Stations	01.10.2023 to 31.12.2023	
	Executed Passes	Successful Passes
All stations (Neustrelitz-Germany, Inuvik-Canada)	231 (33 INU)	230 (33 INU)

Table 7-3 X-Band Ground Station Passes

Work was finalized during Q4 2023 to integrate Inuvik (Canada) as an additional X-Band ground station (S-Band already completed in Q3 2023). After integration, more data and more flexibility in S-band and X-band data reception are expected, especially concerning image acquisitions over Europe. During Q3/2023, EnMAP obtained the license to use the station and the final integration works were resumed (reception and end-to-end tests). By the end of Q4/2023 the X-Band integration and tests were successfully concluded successfully. By the end of 2023, Inuvik station is used for regular S-Band and X-Band operations.

7.4 Processors

[3] provides the product specification and [4], [5], [6], [7] the algorithm theoretical basis for Level 1B, Level 1C and Level 2A (land / water).

In the reporting period (01.10.2023-31.12.2023) there was one processor update:

1. Version 01.04.01 (12.12.2023, available to users on 10.01.2024)

This version includes the following changes:

- Fixed a problem with peaks in snow spectra for L2A Land products
- Fixed a crash occurring for scenes processed in polar projection
- Improved error handling in Screening for scenes with incomplete or unusable VC-AUX files.
- Implemented correction algorithm for SWIR microvibrations (for internal testing, deactivated by default).
- Fixed a minor bug in the across-track destriping algorithm.

The following limitations are applicable as of 30.09.2023:

- The SWIR-A compressor cooler produces a micro-vibration pattern of horizontal stripes on SWIR bands with strong spectral gradients. Still, all spectral and radiometric requirements are within the specification of the mission. The correction is implemented and being tested in V01.04.01, but not active by default.

The following changes are expected to be performed by 31.03.2024:

- Implementation and testing of correction for SWIR along-track striping
- Reduction of fluctuations in L2A-water spectra
- Correct use of turbidity options for L2A-water processing (always clear option used until now)
- Sun-glint mask correction

7.5 Calibrations

Table 7-4 summarizes the radiometric calibration observations acquired in this quarter and which will be described in the rest of this section. The calibration acquisitions were generally acquired according to the routine operations plan. However, due to a couple of mission outages, fewer datatakes were acquired than anticipated.

Category	01.10.2023 to 31.12.2023	
	Number of Archived Observations	Size (in GB)
Total	21	82.7
Deep Space	2	2.6
Rel. Radiometric	10	39
Abs. Radiometric	2	2.6
Linearity	2	34
Spectral Calibration	5	4.5

Table 7-4 Number and size of archived radiometric and spectral calibration observations

The continuous degradation of the VNIR sensor was monitored and quantified. The rate of degradation is constantly decreasing as illustrated in Figure 7-2 and by the end of March 2023 it has reached the point where it is practically negligible and has been kept that way during the reporting period. The effect on the radiometric calibration coefficients of a few selected bands is shown in Figure 7-3.

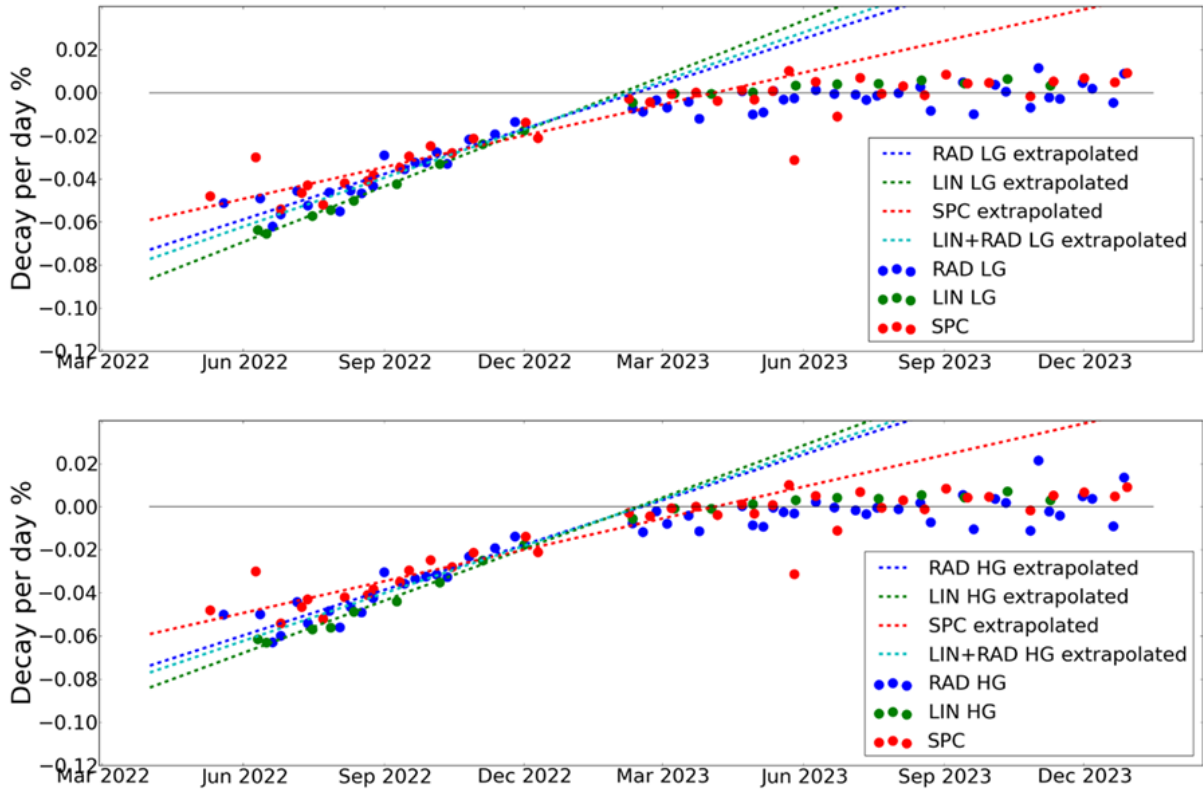


Figure 7-2 Decay per day from Lamp (RAD), Linearity (LIN) and Spectral (SPC) measurements for low gain (top) and high gain (bottom)

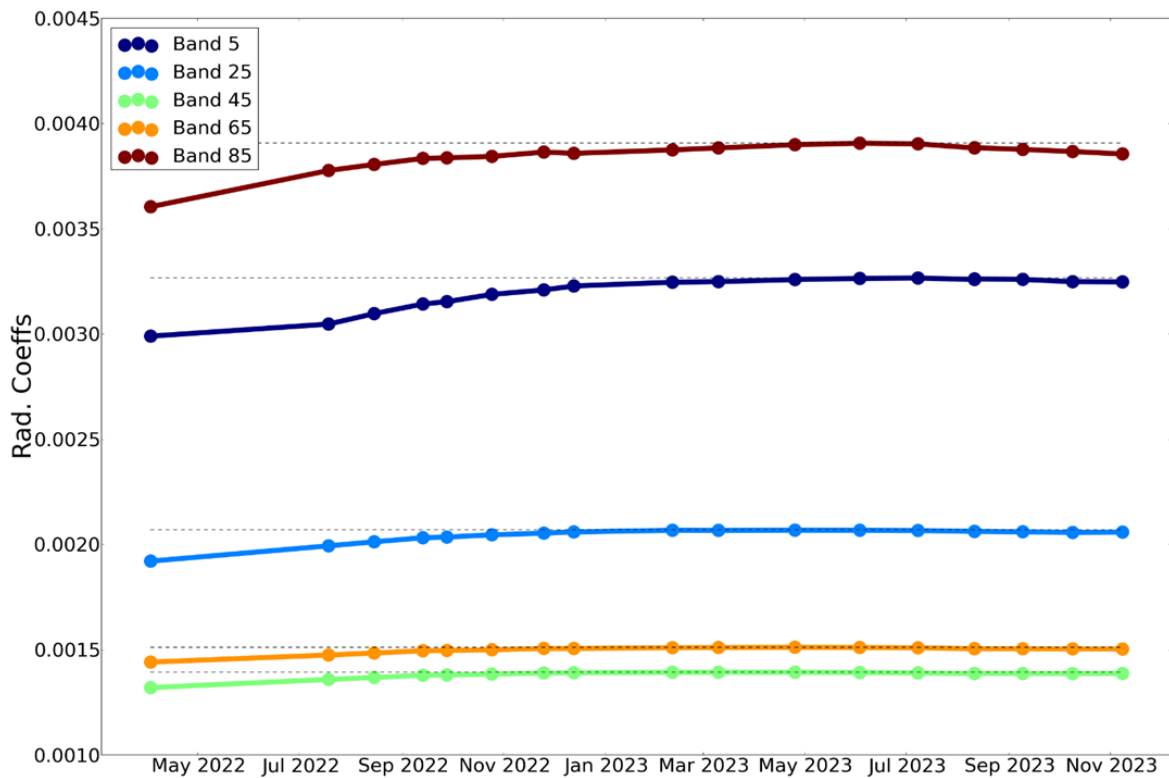


Figure 7-3 Average percentage change in the VNIR radiometric coefficients for five selected bands since launch

7.5.1 Dead Pixels

The following table shows the number and percentage of dead pixels. Figure 7-4 and Figure 7-5 show the position of the dead pixels in the focal plane of VNIR and SWIR sensors respectively. There have been no updates since 31.08.2022.

Defect Pixels	01.10.2023 to 31.12.2023	
	Number of Pixels	Percent
Total	1921	0.8
VNIR	137	0.2
SWIR	1784	1.2

Table 7-5 Number and percent of dead pixels

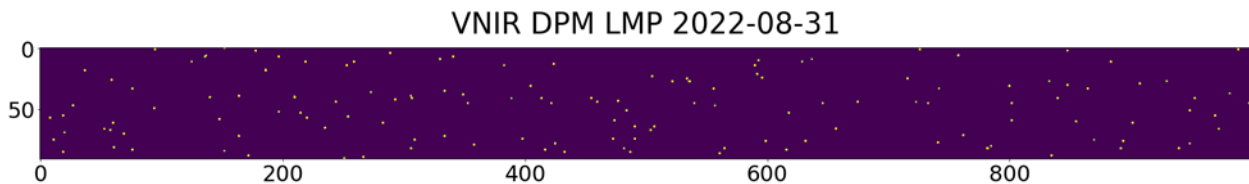


Figure 7-4 VNIR Dead Pixel Mask

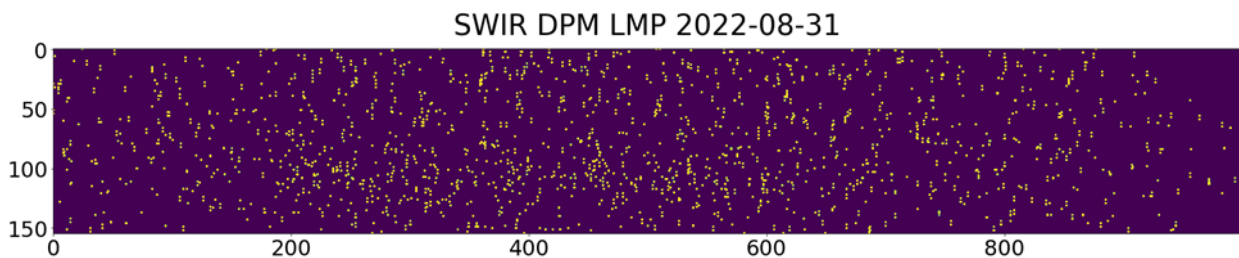


Figure 7-5 SWIR Dead Pixel Mask

There are no clusters of more than three spectrally or spatially adjacent dead pixels.

7.5.2 Spectral Calibration

Remark: In the following figures, OBCA is abbreviation for On-Board Calibration Assembly for spectral and radiometric calibrations.

Category	01.10.2023 to 31.12.2023	
	Number of Archived Observations	Size (in GB)
Total	5	4.5
Spectral Calibration	5	4.5

Table 7-6 Number and size of archived spectral calibration observations

The spectral properties – in particular center wavelength (CW) (see Figure 7-6 and Figure 7-7) and full width at half maximum (FWHM) (see Figure 7-8) for each band (spectral coordinate) and pixel (spatial coordinate) – have been characterized, considering all bands and pixels provided in Level 1B, Level 1C and Level 2A products.

The major conclusions of the monitoring of the spectral performance is summarized as follows:

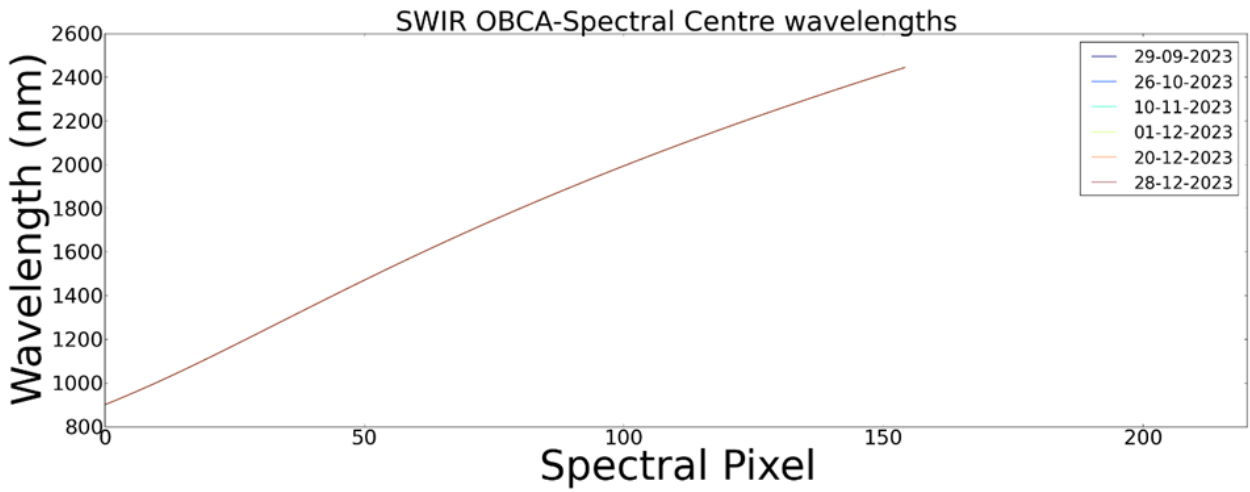


Figure 7-6 VNIR (top) and SWIR (bottom) center wavelength in nm

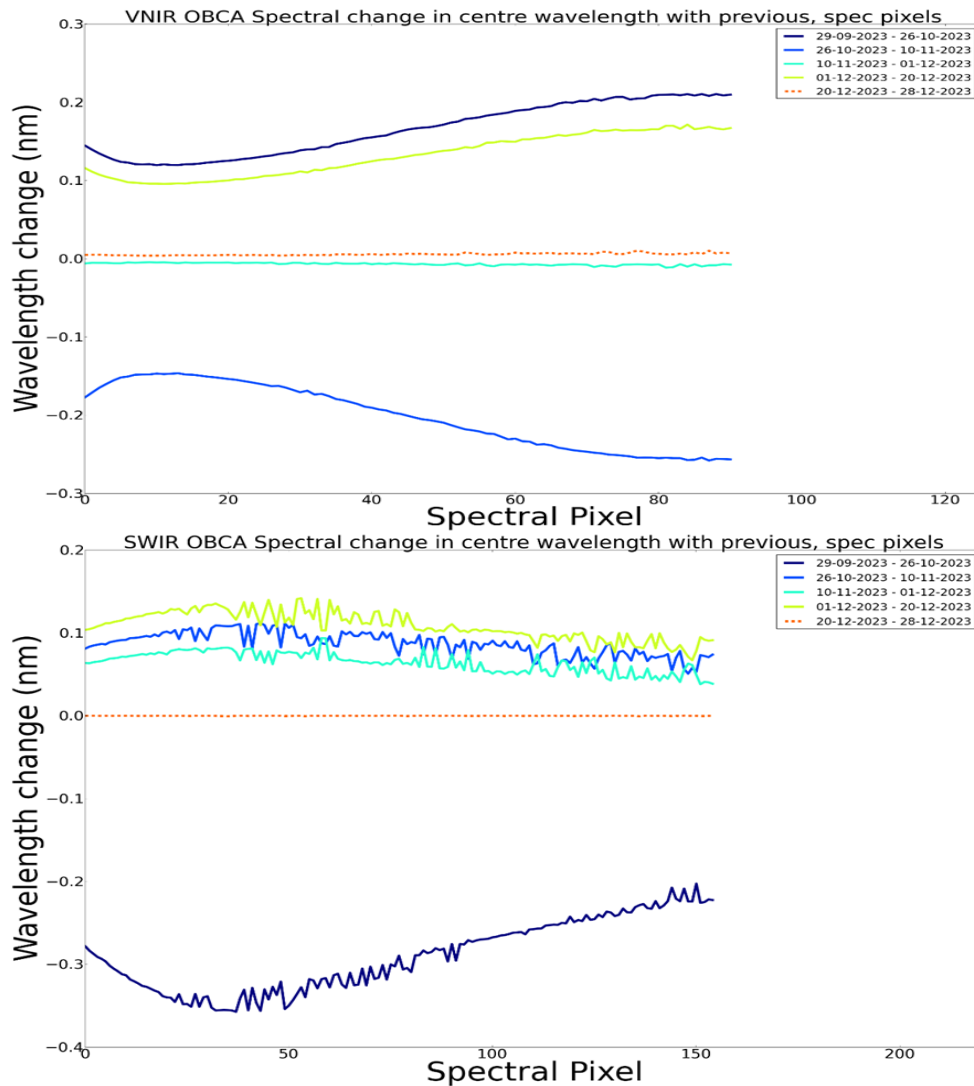


Figure 7-7 Change in center wavelength per spectral pixel for VNIR (top) and SWIR (bottom)

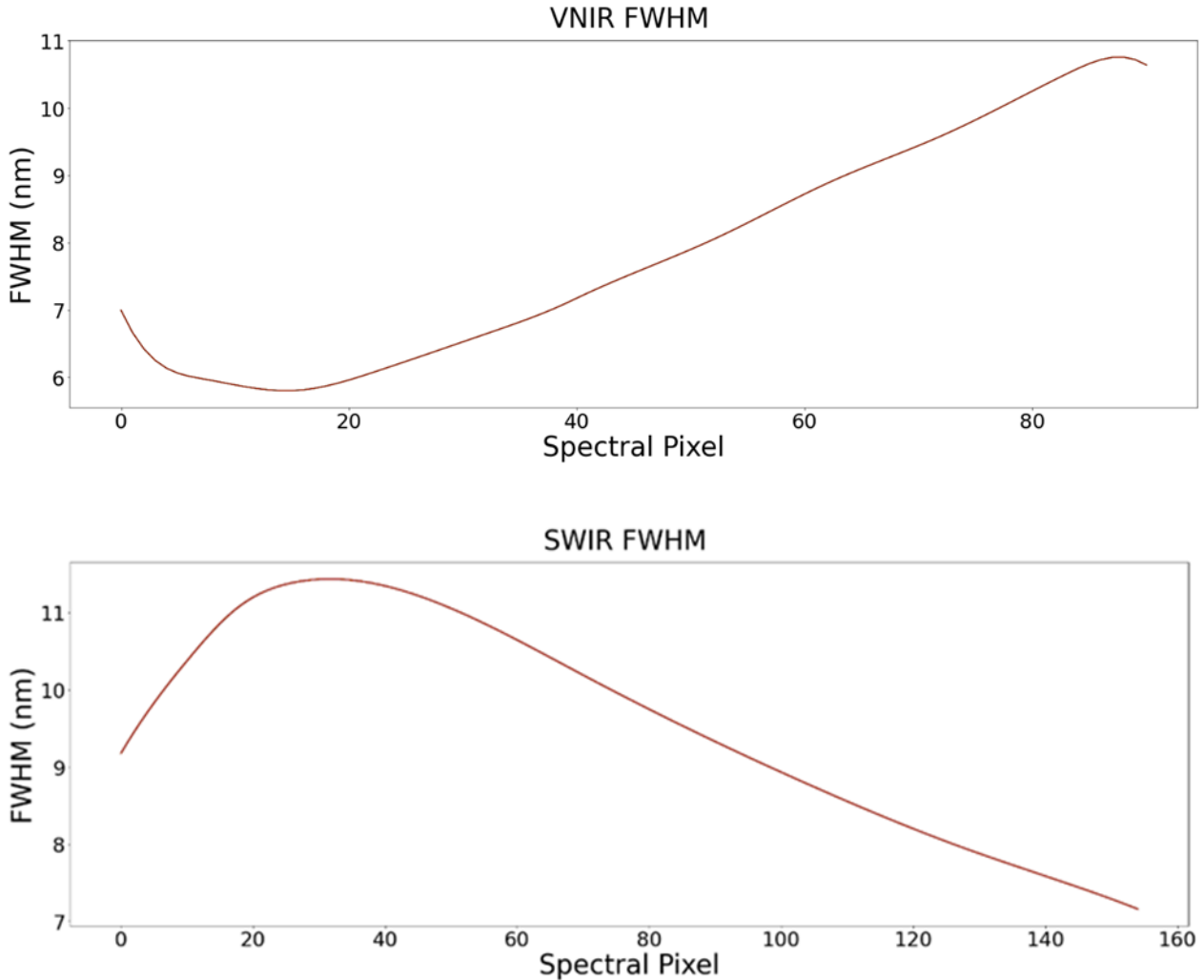


Figure 7-8 VNIR (top) and SWIR (bottom) FWHM in nm

CW and FWHM are available in the spectral calibration tables (see Table 7-7) and System Response Functions (SRF) per band are modelled by a Gaussian shape using those parameters.

No calibration products were generated and delivered during the reporting period.

Product	Type	Date of Generation	Date of Validity Start	Date of Validity End	Delivered to

Table 7-7 Generated spectral calibration tables

7.5.3 Radiometric Calibration

Category	01.10.2023 to 31.12.2023	
	Number of Archived Observations	Size (in GB)
Total	16	78.2



Deep Space	2	2.6
Rel. Radiometric	10	39
Abs. Radiometric	2	2.6
Linearity	2	34

Table 7-8 Number and size of archived radiometric calibration observations

The radiometric properties – characterized in particular by the calibration coefficient for each band (spectral coordinate) and pixel (spatial coordinate) and radiance – during this reporting period are investigated, considering all bands and pixels and radiances provided in Level 1B, Level 1C and Level 2A products.

Both sensors feature two gain settings each. VNIR applies a quantization of 13 bits using a pixel-individual automatic gain switching, where the low gain value is automatically selected, if the signal exceeds a defined threshold. SWIR applies a fixed gain setting, where bands below 1980 nm take the low gain value and bands above 1980 nm take the high gain value.

Radiometric calibration coefficients (see Figure 7-9, Figure 7-10 and Table 7-9) and VNIR RNU (response non-uniformity) (see Figure 7-12) were affected by the degradation of the VNIR sensor during commissioning but have stabilized from Q1 2023. In-flight, the gain matching coefficients (see Figure 7-11), the SWIR calibration coefficients, and the SWIR RNU (response non-uniformity) (see Figure 7-12) have been stable.

During the reporting period, 2 Absolute Radiometric calibration measurements were obtained. These took place on: 09.10.2023 and 08.11.2023. Owing to the initial degradation in the VNIR sensor during commissioning, new calibration and reference tables were created for each new absolute radiometric measurement. Although the VNIR degradation has almost stopped, the overall effects are visible in the reference measurements of the sun. However geometric conditions (sun-earth distance, pointing angle) also play a role in the absolute magnitude so the degradation cannot be quantified with these reference measurements.

The major conclusions of the monitoring of the absolute performance is summarized as follows:

- Changes in the VNIR sensor have affected the absolute Radiometric calibration coefficients: the increasing signal in the VNIR sensor, although not homogeneous, has resulted in decreasing radiometric coefficients. In this reporting period, the calibration coefficients decreased by about -0.12% to offset the increase in absolute signal, relative to the sun calibration on 09.09.2023 (Figure 7-9 and Figure 7-10). Regarding RNU, the degradation features are still visible in the focal plane. Looking at the average along across track pixels, the RNU correction appears to have changed slightly in this reporting period (Figure 7-12). Lastly, the Gain Matching correction has been relatively stable during this reporting period (Figure 7-11).
- The SWIR sensor has shown good stability during this reporting period, with no significant changes in the gain matching, RNU or radiometric calibration coefficients (Figure 7-9 and Figure 7-10).
- Regarding the total change in calibration corrections as a result of the VNIR degradation, almost all pixels experienced a change of less than 2.5% between consecutive measurements as set in requirement [HSI-POSR-0410]. The only pixels which exceeded this value were already marked as dead during inflight assessment. No SWIR pixels experienced a change of more than 2.5% between consecutive absolute calibration measurements.
- New VNIR and SWIR calibration and reference tables were created for both absolute radiometric measurements, mainly due to the changes in the VNIR sensor. The VNIR radiometric calibration coefficients have decreased in this reporting period to offset the increasing VNIR signal. The changes are small, and within requirements, so the dynamic coefficients are not calculated and calibration coefficients are taken directly from the most recent calibration table as envisioned at the beginning of the mission. Monthly updates to the radiometric calibration table may not be necessary if the coefficients settle in a steady state.

Even though the EnMAP radiometric quality was well within the requirements, the absolute calibration measurements were taken at monthly intervals. Changes between measurements are comparable to the SWIR sensor. It is planned to perform calibration acquisitions at longer time intervals in the future.

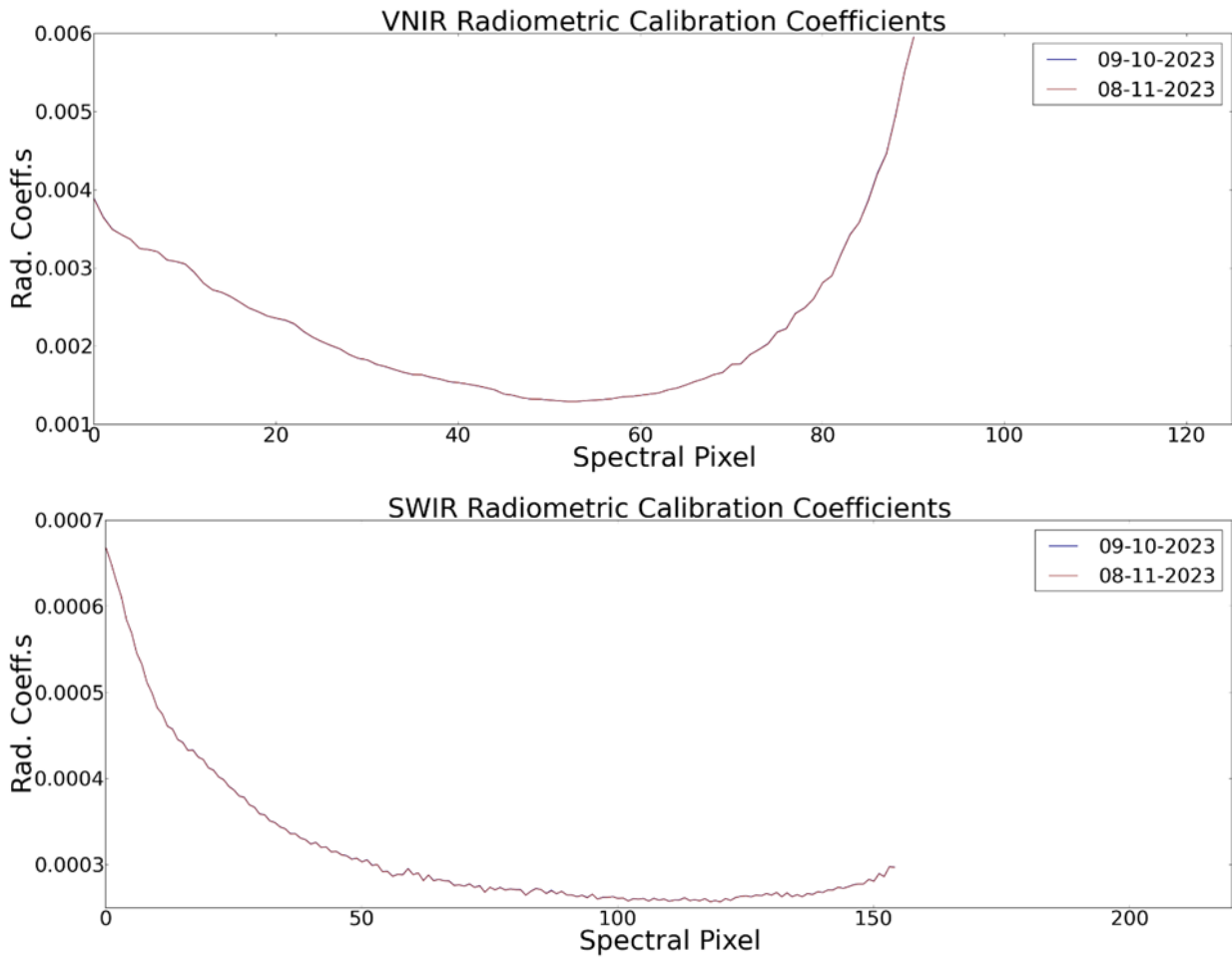
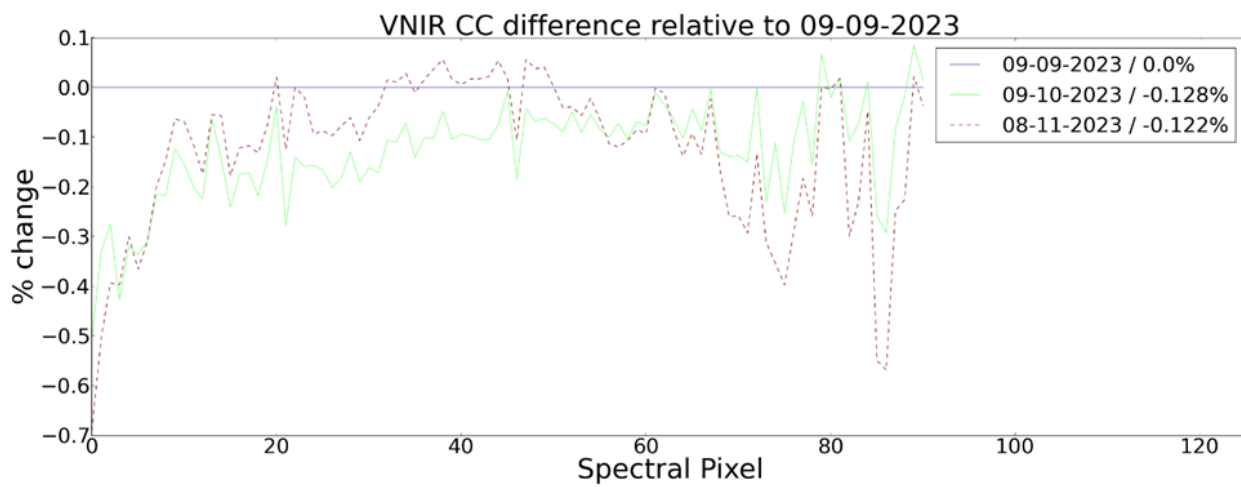


Figure 7-9 VNIR (top) and SWIR (bottom) calibration coefficient in $mW/cm^2/sr/\mu m$



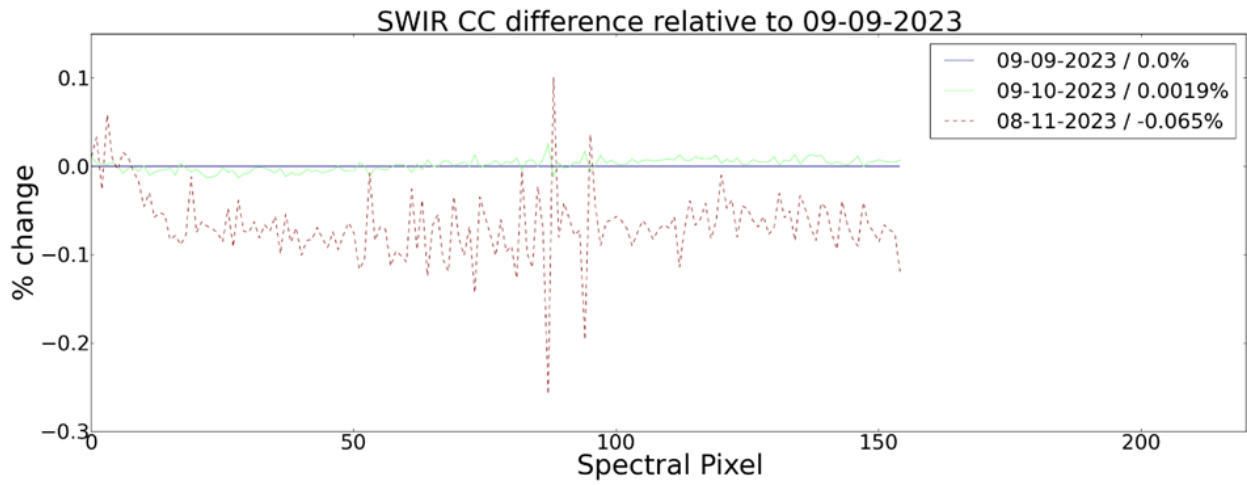


Figure 7-10 Percentage change in VNIR Calibration Coefficients (top) and SWIR Calibration Coefficients (bottom)

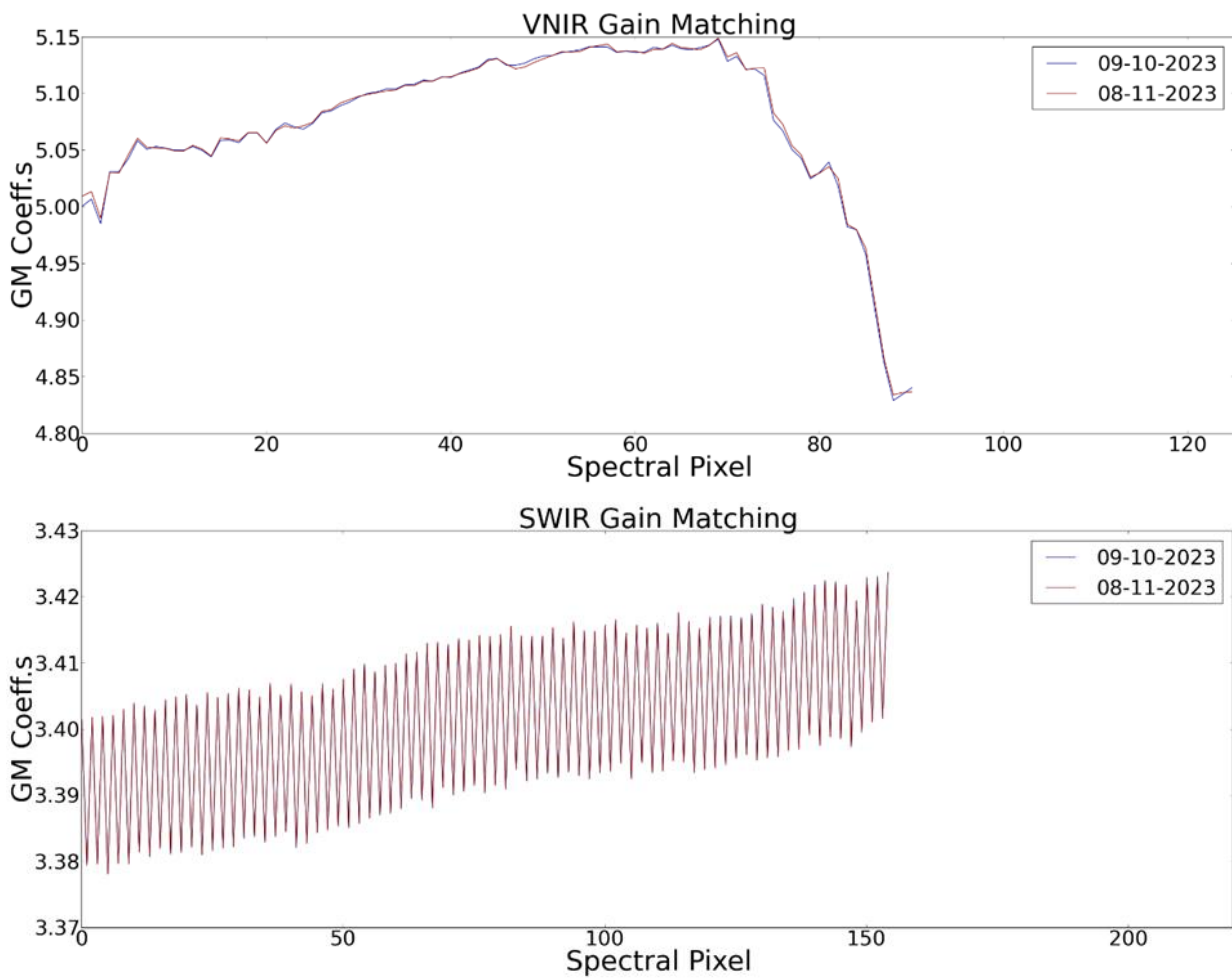


Figure 7-11 VNIR (top) and SWIR (bottom) gain matching calibration coefficients

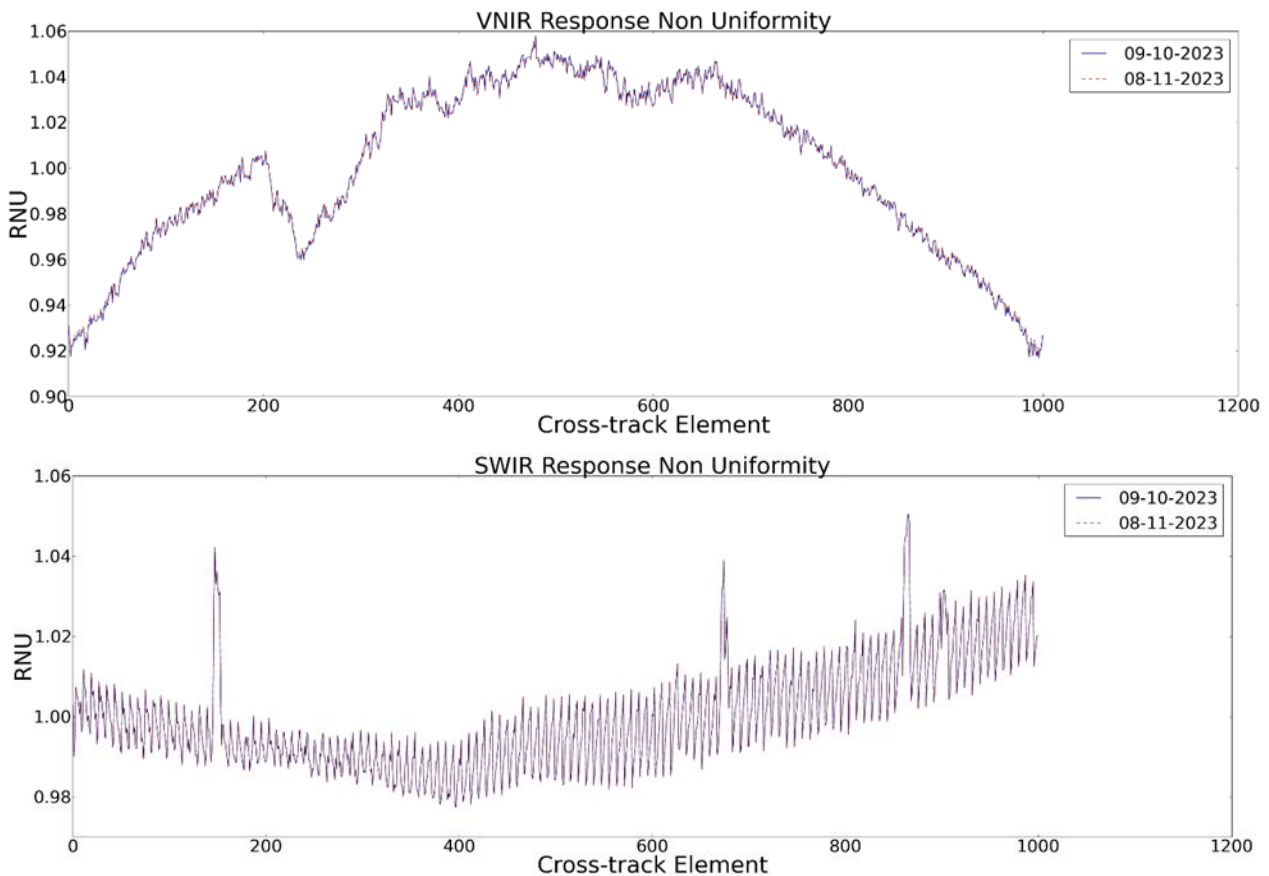


Figure 7-12 VNIR (top) and SWIR (bottom) response non-uniformity coefficients

The Signal-to-Noise Ratio (SNR) is derived from the Linearity reference measurements. This is not a perfect set-up for the assessment of the SNR as the linearity measurements only cover a single wavelength and light level at increasing integration times. However, it is well constrained, covering a wide range of radiances including the levels of the solar reference spectrum (30% reflectance, 30° sun incidence angle, 21 km visibility, target 500 m above sea level). The lamp reference measurements are not used, as the reference spectrum is not well covered at the radiances of the lamp and extrapolation would be required to test the performance at the SNR requirements: SNR greater than 500 at 495 nm in VNIR for the solar reference spectrum value; and SNR greater than 150 at 2200 nm in SWIR for the reference spectrum.

For the VNIR sensor, SNR is computed from the linearity calibration measurement. SNR values are shown as a contour map with the solar reference spectrum (30% reflectance, 30° sun incidence angle, 21 km visibility, target 500 m above sea level) as a blue line. Contour lines with SNR values of 150 and 500 are also shown in black. A similar plot for the low gain mode including the position of the requirement [HIS-POSR-0010] which is marked with a black cross.

For the SWIR sensor, SNR is also computed from the linearity calibration measurement. SNR values for the high gain mode are shown as a contour map with the solar reference spectrum (30% reflectance, 30° sun incidence angle, 21 km visibility, target 500 m above sea level) as a blue line and the position of the requirement [HIS-POSR-0010] is marked with a black cross. Contour lines with SNR values of 150 and 500 are also shown in black.

The calculation of the SNR from the onboard linearity calibration changed during this reporting period. Previously, outlier frames were excluded from the initial L0 datacube based on statistical filtering. Following an analysis of the L0 cube, the filtering was removed since there were so few outlier frames. As a result, the SNR estimation has changed and the results have decreased since the last reporting period. Nevertheless, the SNR performance of EnMAP exceeds the requirements. At the position of the requirement, the SNR exceeds 500 with a value of 596 for VNIR and exceeds 150 with a value of 199 for SWIR (values normalized to 10 nm equivalent bands, as defined in the requirement formulation).

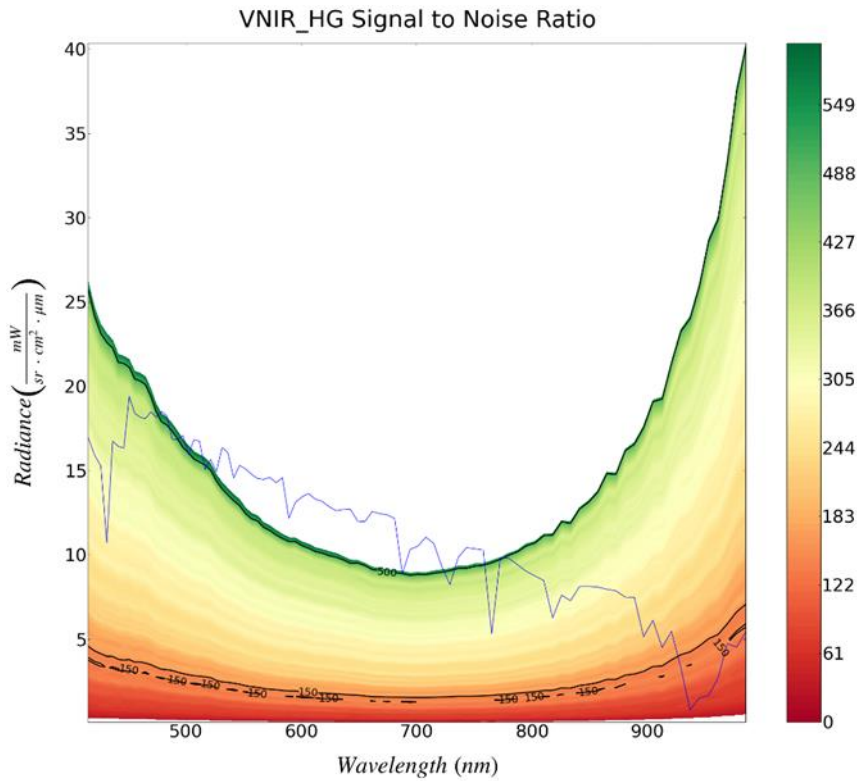


Figure 7-13 SNR contour map for VNIR high gain from the LED linearity observations observed on 08.11.2023. The solar reference spectrum is shown with a blue line. Contour lines with SNR values of 150 and 500 are also shown in black.

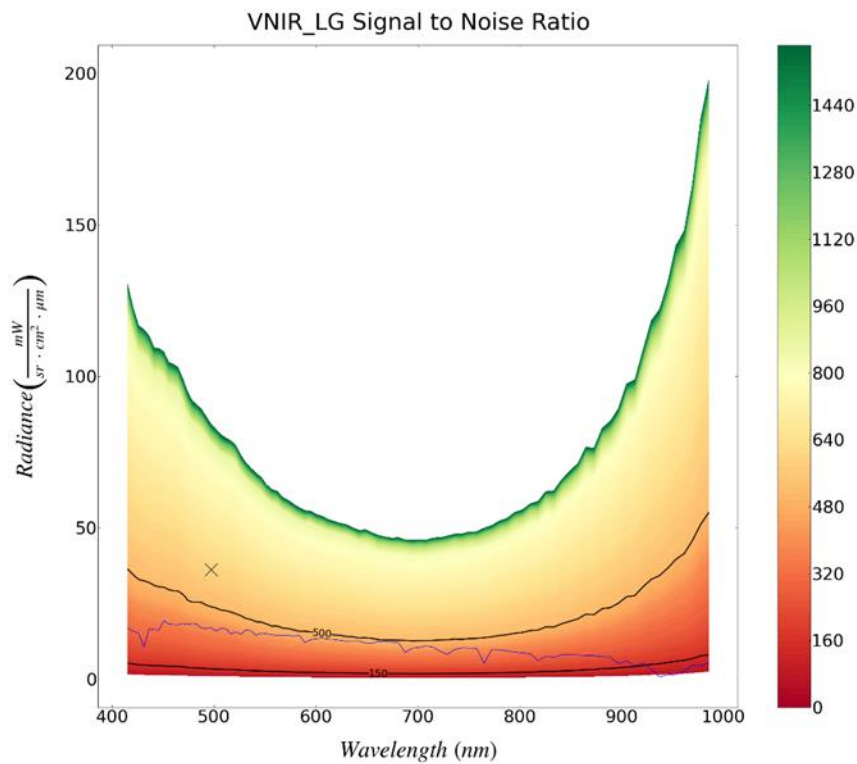


Figure 7-14 SNR contour map for VNIR low gain from the LED linearity observations observed on 08.11.2023. The solar reference spectrum is shown with a blue line and the position of the requirement is marked on the reference spectrum with a black cross. Contour lines with SNR values of 150 and 500 are also shown in black.

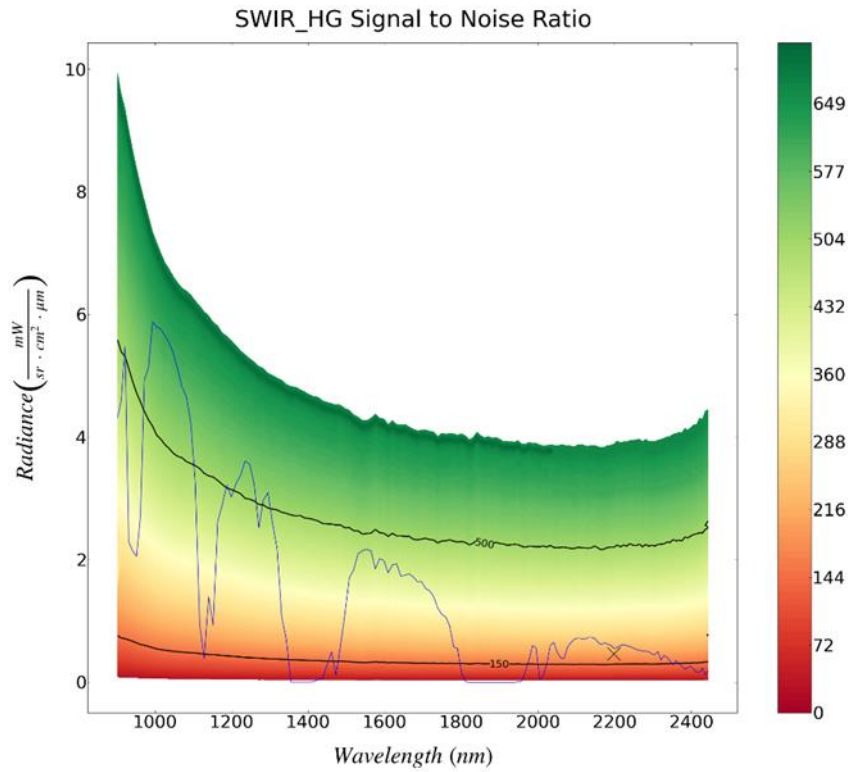


Figure 7-15 SNR contour map for SWIR high gain from the LED linearity observations observed on 08.11.2023. The solar reference spectrum is shown with a blue line and the position of the requirement is marked on the reference spectrum with a black cross. Contour lines with SNR values of 150 and 500 are also shown in black.

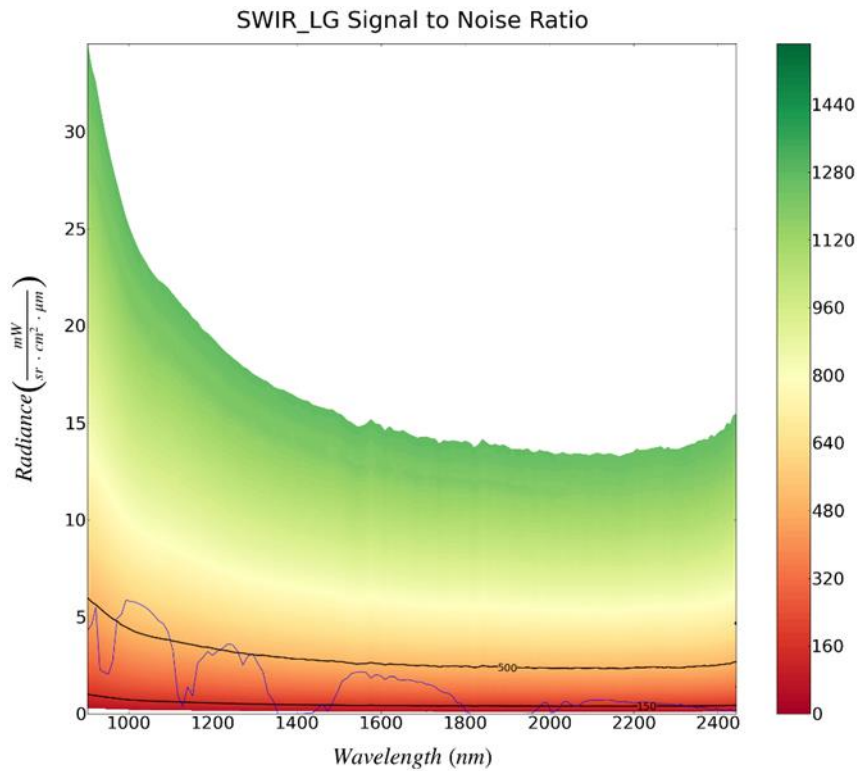


Figure 7-16 SNR contour map for SWIR low gain from the LED linearity observations observed on 08.11.2023. The solar reference spectrum is shown with a blue line. Contour lines with SNR values of 150 and 500 are also shown in black.

The following calibration products were generated and delivered:

Product	Type	Date of Generation	Date of Validity Start	Date of Validity End	Delivered to
ENMAP01-CTB_RAD-20231019T000000Z_V040005_20231010T111642Z	CTB_RAD	10.10.2023	19.10.2023	18.11.2023	DIMS
ENMAP01-CTB_RAD-20231118T000000Z_V040005_20231109T134508Z	CTB_RAD	09.11.2023	18.11.2023	-	DIMS
ENMAP01-REF_SUN-20231019T000000Z_V040005_20231010T111642Z	REF_SUN	10.10.2023	19.10.2023	18.11.2023	DIMS
ENMAP01-REF_SUN-20231118T000000Z_V040005_20231109T134508Z	REF_SUN	09.11.2023	18.11.2023	-	DIMS

Table 7-9 Generated radiometric calibration tables

7.5.4 Geometric Calibration

There have been no new geometric calibration tables generated in the reporting period.

Type of Calibration Table	ID of Calibration Table	Date of Generation	Date of Validity Start	Date of Validity End
None				

Table 7-10 Generated new geometric calibration tables

The performance of the geometric calibration table is assessed in chapter 7.6.3.

7.6 Internal Quality Control

7.6.1 Archive

Within the given time period (2023-10-01 and 2023-12-31), 943 datatakes with a total of 7419 tiles were acquired and archived (remark: additional datatakes acquired during this period but for which the archiving is pending might be missing in the statistics).

The overall quality rating statistics are listed in Table 7-11, and in relation to the Solar Zenith Angle (SZA) in Table 7-12. Also these ratings are further detailed for the VNIR and SWIR detector in Table 7-13, showing a nominal performance rating for the given quality thresholds.

In addition, the rating for the atmospheric conditions for the scenes are depicted in Table 7-14. When setting the atmospheric quality rating in relation to the illumination conditions (i.e., large SZA) during data acquisition (Table 7-15), 27% of the “reduced quality” ratings and over 30% of the “low quality” ratings can be related to low Sun angles / night time acquisitions. This increase can be explained as more acquisitions were taken in the northern hemisphere where during winter unfavourable illumination conditions apply.

In addition, the “low qualityAtmosphere” rating can be further related to high cloud cover (55% of the low qualityAtmosphere tiles) and the unavailability of enough DDV pixels (74%) (see Table 7-16). Consequently, the rating is absolutely reasonable and can be explained.

Parameter	Value	Percentage	Number of tiles
overallQuality	Nominal	98,2%	7284
	Reduced	<1%	1
	Low	1,8%	134

Table 7-11 Overall quality rating statistics

Parameter	Number of tiles	Sub-Parameter	Number of tiles
overallQuality = Low	134		
		Thereof with SZA > 70°	134

Table 7-12 Overall quality rating in relation to Sun Zenith Angle (SZA)

Parameter	Number of tiles	Sub-Parameter	Number of tiles
overallQuality = Reduced	1		
		Thereof with qualityVNIR nominal	0
		Thereof with qualitySWIR nominal	1
overallQuality = Low	134		
		Thereof with qualityVNIR nominal or reduced	3
		Thereof with qualitySWIR nominal or reduced	134

Table 7-13 Reduced and low quality rating statistics

Parameter	Value	Percentage
QualityAtmosphere	Nominal	27%
	Reduced	17%
	Low	57%

Table 7-14 QualityAtmosphere rating statistics

Parameter	Number of tiles	Sub-Parameter	Number of tiles
overallAtmosphere = Reduced	1244		
		Thereof with SZA > 60°	336
		Thereof with SZA > 70°	61
		Thereof with SZA > 80°	18

overallAtmosphere = Low	4225
Thereof with SZA > 60°	1277
Thereof with SZA > 70°	467
Thereof with SZA > 80°	221

Table 7-15 QualityAtmosphere rating in relation to Sun Zenith Angle (SZA)

Parameter	Number of tiles	Sub-Parameter	Number of tiles
overallAtmosphere = Low	4425		
		Thereof with Cloud Cover > 66%	2318
		Thereof with DDV warnings	3141

Table 7-16 QualityAtmosphere rating in relation to Cloud Cover and DDV availability

7.6.2 Level 1B

7.6.2.1 Radiometric Performance

Defective / de-calibrated detector elements

Using the Detector Map components, an offline check of possibly defective or de-calibrated detector elements is conducted. In particular, a detector element is identified as “possibly defective” if it is suspicious in at least 75% of the useful tiles. Note that this analysis is based on L1B_RAD data, so no dead / defective pixel interpolation was carried out. Within the given reporting period, the following indications for defective pixels are found for the VNIR and the SWIR camera:

VNIR (total of 7419 tiles, with 7286 suitable for analysis):

Newly found suspicious pixels in **green**, previously detected in **black**, no longer present ones in **red**.

Band	Cross-track element
------	---------------------

77	600
---------------	----------------

85	14
----	----

89	395
----	-----

Note that the band index starts at 1.

SWIR (total of 7419 tiles, with 7223 suitable for analysis):

Newly found suspicious pixels in **green**, previously detected in **black**, no longer present ones in **red**.

NOTE: due to the change in SWIR band configuration within the previous period Q3 (see EN-GS-RPT-1803 Issue 5), the band index from band 45 till 75 did change by +1 (with bands 45, 74 & 75 newly added). Thus, in the following, the new band numbers are given, while the colour index is adjusted in order to account for real changes.

Band	Cross-track element
------	---------------------

Band	Cross-track element
------	---------------------



1	817	48	511	96	341, 819
2	235, 286, 593, 673	49	218	100	513 (previously detected)
3	381	50	311, 344, 395	101	318
4	362, 363, 418	51	154, 155	102	925
5	687	53	97, 98	106	107
7	910	54	602 , 941	107	265, 764
8	801	56	221, 965	108	886
8	124	58	632, 922	111	315
11	715	59	89, 90	118	837
14	29, 684	61	312		
16	535	63	123		
19	84	66	93		
20	766	49	864		
29	855, 928	72	801, 844, 845		
30	360	75	737		
31	360	85	525		
33	560	89	285		
38	241	91	973		
39	486	92	677, 973		

Dead detector elements

Within the given reporting period, the statistics for dead pixels are provided in Table 7-17 and Table 7-18. When comparing these numbers to the estimates in the EN-GS-RPT-1702 Radiometric Calibration Report, one must bear in mind that the latter is based on the full detector readout configuration, while the numbers provided in the following are related to the standard readout configuration as provided in the user product. Because of the smaller readout area, these following dead pixel numbers are lower in comparison.

Parameter	Number of dead pixels	Percentage of tiles in reporting period
DeadPixelsVNIR	137	100%

Table 7-17 Dead pixel statistics, VNIR

Parameter	Number of dead pixels	Percentage of tiles in reporting period
DeadPixelsVNIR	1509	100%

Table 7-18 Dead pixel statistics, SWIR

Saturation and radiance levels

Within the given reporting period, no indications for increased saturation defects are found for the VNIR and the SWIR camera (see Table 7-19 and Table 7-20).

Parameter	Value (per mille of scene)	Percentage of tiles
SaturationCrosstalkVNIR	0	90%
	> 0 per mille	10%
	> 10 per mille	2%

Table 7-19 Saturation statistics, VNIR

Parameter	Value (per mille of scene)	Percentage of tiles
SaturationCrosstalkSWIR	0	91%
	> 0 per mille	9%
	> 10 per mille	0.5%

Table 7-20 Saturation statistics, SWIR

Other radiometric artifacts

Within the given reporting period, the striping performance is similar to the one encountered during the Commissioning Phase. Within PCV, different de-striping approaches were tested, and the selected one by M. Brell (GFZ) is implemented in processor version V010200 (07.03.2023).

Apart from this, no indications for an increase in general radiometric artifacts are found for the VNIR and the SWIR camera (see following tables).

Parameter	Value (number of pix)	Percentage of tiles
generalArtifactsVNIR	0	0%
	> 0	100%
	> 10	6%
	> 100	2%
	> 1000	0%

Table 7-21 Artifacts statistics (without striping), VNIR

Parameter	Value (number of pix)	Percentage of tiles
generalArtifactsSWIR	0	0%
	> 10	100%
	> 25	8%
	> 100	2%
	> 1000	0%

Table 7-22 Artifact statistics (without striping), SWIR

7.6.2.2 Spectral Performance

For the analysis of the spectral stability, the Detector Maps of all Earth datatakes acquired in the reporting period were used. Note that no smile correction was applied, so the analysis shows only on the instrument characteristics. At the wavelengths of stable atmospheric features (760 nm Oxygen absorption and CO2 absorption at ~2050 nm), simulations of spectral shifts were carried out by resampling the absorption in the interval of +/- 3.0 nm with steps of 0.05 nm. Then the signal of the Detector Maps and the simulated shifted absorptions were normalized, and a least-square fit was used where the sensed absorption matches the simulations. Also an additional polynomial fitting was applied, as especially the CO2 absorption band region has low signal and is thus significantly influenced by noise.

When repeating this analysis for many Detector Maps, then the spectral behavior over time can be addressed (Figure 7-17, Figure 7-18). More important is the standard deviation of the shift, as this represents the spectral stability within the given period [AR-5]. As shown in Figure 7-17 and Figure 7-18 the standard deviation (1σ) at 760 nm is better than 0.20 nm for all cross-track elements, and better than 0.60 nm in the 2050 - 2060 nm region. Also the cross-track shape shows little variation; in case of the VNIR, the stability is equally good for all cross-track elements, while for the SWIR the shape is similar to the detected center wavelengths (CW) deviation.

In summary, these findings agree well with the instrument performance estimated during the Commissioning Phase [IR-01] and previous QC reports.

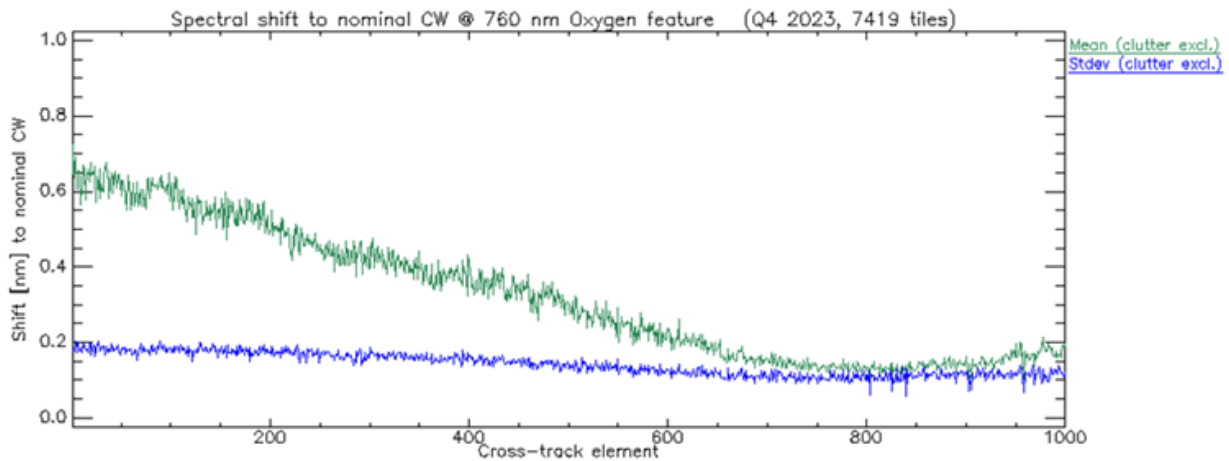


Figure 7-17 VNIR estimated spectral shift at 760 nm w.r.t the nominal band center, and relative spectral stability expressed at 1 sigma (Q3 2023)

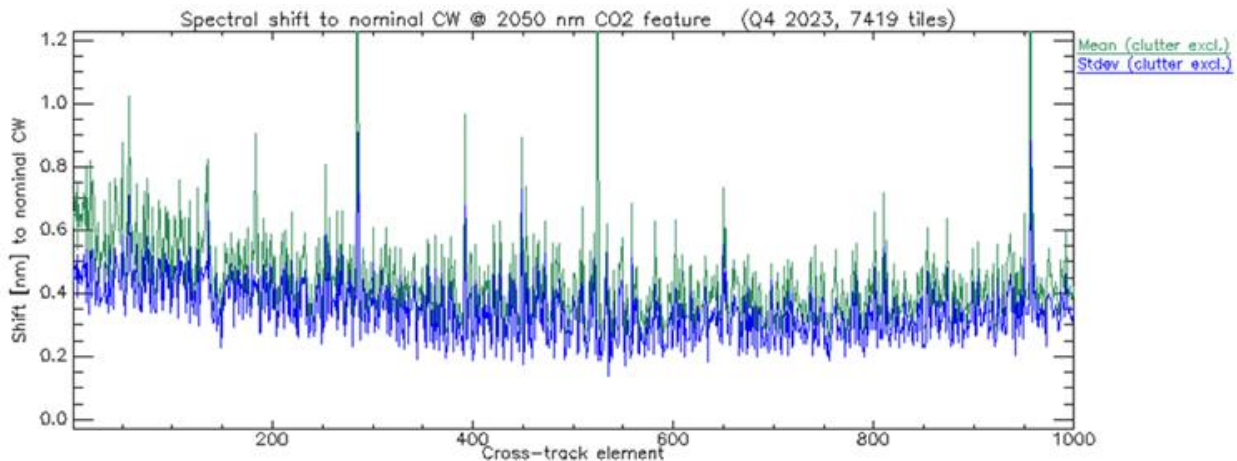


Figure 7-18 SWIR estimated spectral shift at 2050 nm w.r.t the nominal band center, and relative spectral stability expressed at 1 sigma (Q3 2023)

In addition, the spectral shifts were also estimated against the related in-orbit spectral calibration table CTB_SPC. For this analysis, the reference is thus not the nominal center wavelengths (i.e., a single number per band), but the CW per cross-track pixel, thus explicitly including the spectral smile (see Figure 7-19).

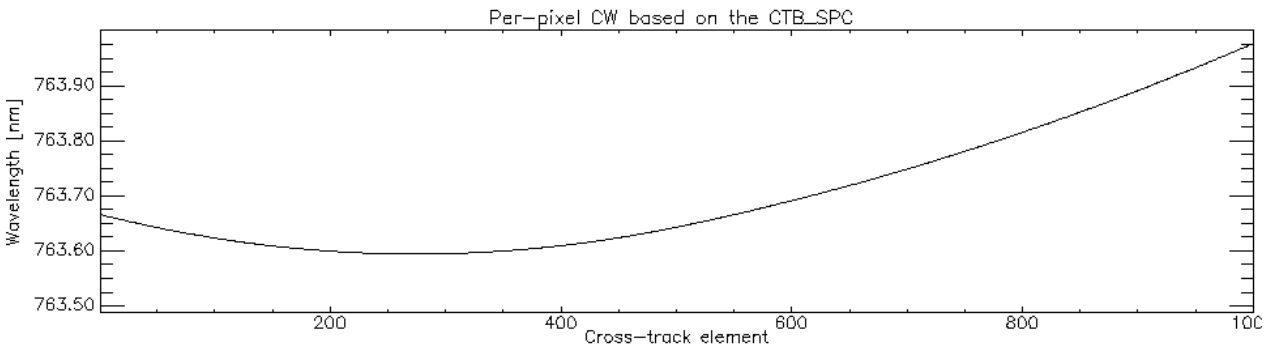


Figure 7-19 Center wavelengths per cross-track pixel based on the spectral calibration table (VNIR band 62).

When aggregating the shifts (Figure 7-20), as expected the mean derivation is now almost constant in across-track direction and below 0.4 nm, underpinning the validity of the in-orbit spectral calibration. The variability expressed as the standard deviation at 1 sigma rarely exceeds 0.2 nm, which is -as expected- in agreement with the analysis using a single CW. Note that the differences in scatter are due a slightly different matching, but are within the general uncertainty of the method.

Additionally, in order to further demonstrate that the mean derivation to the CTB_SPC is within the spread of the data, the mean and standard deviation are also calculated using the relative values. The mean over all detector map fits is shifted by ~ 0.5 nm towards shorter wavelengths, but given the spread of the data (expressed as ± 1 standard deviation in the plot) this derivation is within the variations of the used Earth datatakes and within the limitations of the method.

In summary, for the VNIR the differences to the CTB_SPC are within the spread of the data and in the accuracy of the method, confirming the validity of the spectral calibration.

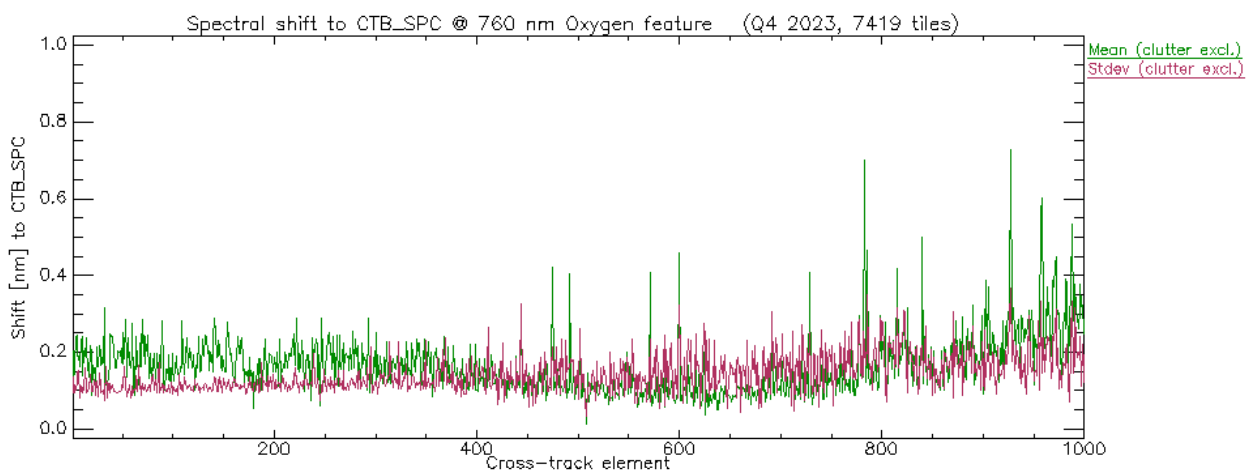


Figure 7-20 VNIR estimated spectral shift at 760 nm w.r.t the valid spectral calibration table (CTB_SPC), and relative spectral stability expressed at 1 sigma (Q4 2023, 7419 tiles)

For the SWIR having less pronounced atmospheric absorption features, more influence of the background and a much lower signal level, the fitting also results in more clutter. Also there is now an increased number of DMs where no fit was achieved. Nevertheless, considering the EnMAP bandwidths of ~ 8.5 nm (FWHM), the spread of the vast majority of successful fits is within 3 nm, which agrees with the estimated stdev of ~ 0.6 nm (1 sigma) shown in . Note that the bi-modal distribution in the histograms is currently under investigation.

In order to show that the mean derivation to the CTB_SPC is within the spread of the data, also the mean and standard deviation are calculated using the relative values, as shown in Figure 7-22. Here the differences to the CTB_SPC are well within 1 standard deviation, confirming the validity of the spectral calibration.

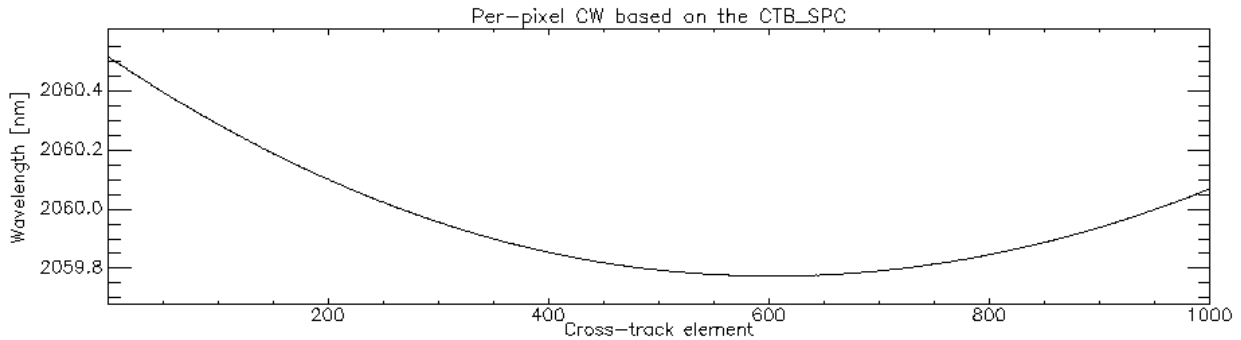


Figure 7-21 Center wavelengths per cross-track pixel based on the spectral calibration table (SWIR band 86).

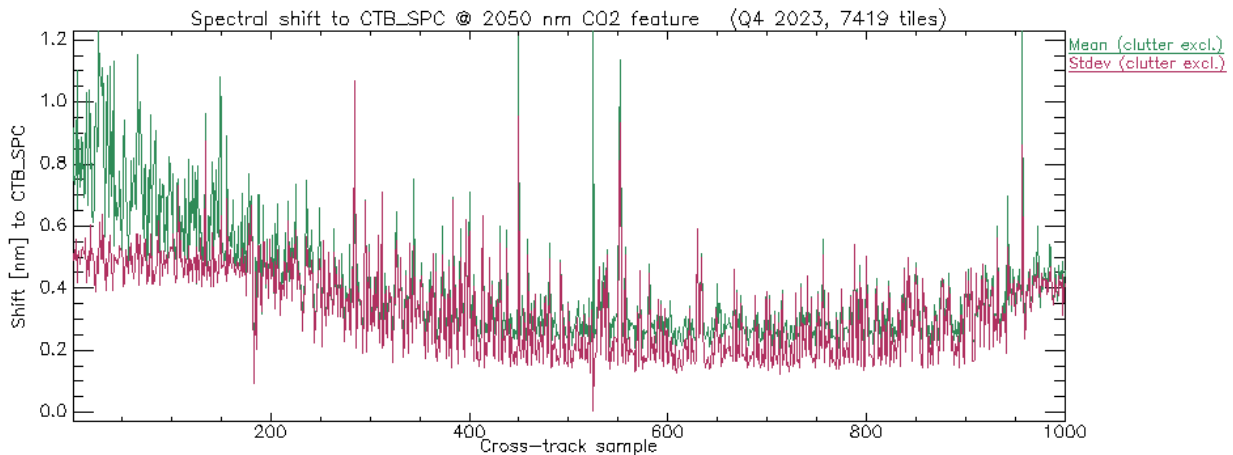


Figure 7-22 SWIR estimated spectral shift at 2050 nm w.r.t the valid spectral calibration table (CTB_SPC), and relative spectral stability expressed at 1 sigma (Q4 2023, 7419 tiles)

To summarize, the alternative fitting approach for the VNIR and SWIR is consistent to the previous approach shown at the beginning of this section, and agrees with previous estimates for the spectral stability of EnMAP.

7.6.2.3 Routine check of scenes in context of updates in CTB_RAD, CTB_SPC calibration tables

7.6.2.3.1 CTB_RAD

Table 7-23 Validated CTB_RAD

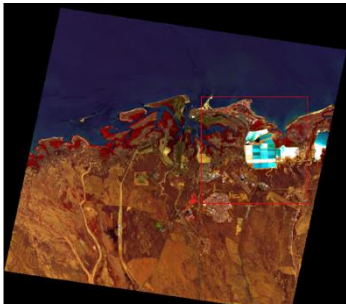


Validated CTB	ENMAP01-CTB_RAD-20231019T000000Z_V040005_20231010T111642Z
Datatake used	ENMAP01-_____L0-DT0000045275_20231003T030028Z_002
	

	Figure 7-23 Datatake used (North Australia)
Summary of result	<p>New CTB_RAD confirmed</p> <ul style="list-style-type: none"> • VNIR: for the given scene, <ul style="list-style-type: none"> • relative changes to P24 are now larger (-0.1% - -0.2%), with more pronounced changes towards shorter wavelengths • absolute change for all bands indicates a higher sensitivity as P24 (i.e., „recovery“) • for the given scene, fringing has again a stronger influence • also the „fingerprint“ (relatively stable region) is now visible again • SWIR: for the given scene: <ul style="list-style-type: none"> • relative change to P24 is again very small, < 0.05% for low and high gain regions • for given scene, SWIR fringing is not visible
Validated CTB	ENMAP01-CTB_RAD-20231118T000000Z_V040005_20231109T134508Z
Datatake used	<p style="text-align: center;">ENMAP01-_____L0-DT0000048472_20231030T190325Z_003</p>  <p style="text-align: center;">Figure 7-24 Datatake used (US Westcoast)</p>
Summary of result	<p>New CTB_RAD confirmed</p> <ul style="list-style-type: none"> • VNIR: for the given scene, <ul style="list-style-type: none"> • relative changes to P21 are again small, below 0.15% in most part of the VIS and NIR • For the given scene, the standard deviation of change is increased above band 80 w.r.t last periods, but mean is as expected • Also single pixel radiance spectra at various brightness levels are as expected. • absolute change is fluctuating about zero, • for the given scene, fringing has only a very minor influence • for given scene, differences are slightly higher at center than towards edges of detector • as before, differences between calibrations are way smaller compared to those early in the mission • SWIR: for the given scene: <ul style="list-style-type: none"> • relative change to P25 is small, < 0.11% for low and high gain regions, but slightly higher than previously • band-to-band changes are slightly larger than for previous periods • for given scene, SWIR fringing is not visible

7.6.2.3.2 CTB_SPC

Table 7-24 Validated CTB_SPC

Validated CTB	ENMAP01-CTB_SPC-20231117T000000Z_V040005_20231114T082347Z
Datatake used	<p style="text-align: center;">ENMAP01- L0-DT0000051370_20231119T174311Z_002</p>  <p style="text-align: center;">Figure 7-25 Datatake used (Memphis, USA)</p>
Summary of result	<p>New CTB_SPC confirmed</p> <p>VNIR:</p> <ul style="list-style-type: none"> • Changes between current and new CTB_SPC are minimal • For given scene & bands, new table is marginally better • Note: For given scene, the spread of the fitting is larger on the left part of the FOV, very likely due to scene properties <p>SWIR:</p> <ul style="list-style-type: none"> • Changes between current and new CTB_SPC are minimal • For given scene & bands, new table is marginally better • Note: For given scene, the spread of the fitting is larger on the left part of the FOV, very likely due to scene properties

7.6.3 Level 1C

This report covers the timeframe between 01.10.2023 and 31.12.2023. No geometric calibration was performed during this period.

In the timeframe of this report, 943 datatakes have been acquired. In 584 of those datatakes (~62 %), enough GCPs and ICPs were found to perform a geometric accuracy assessment. The datatakes without enough GCPs were not assessed quantitatively, but a random subset of them was inspected visually. The vast majority of those datatakes was either almost fully covered with clouds or showing only water, desert or rain forest. The behavior is thus as expected.

The assessment of the RMSE values in the metadata is shown below in Figure 7-26.

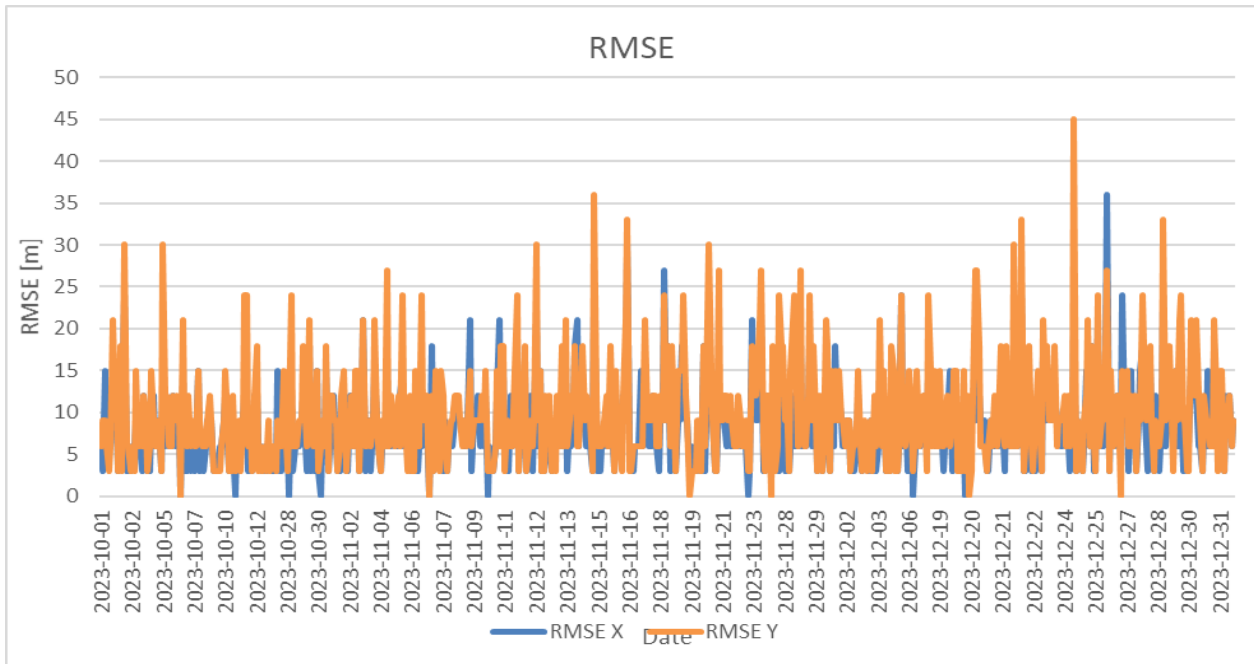


Figure 7-26 Assessment of RMSE values, calculated based on found ICPs, for all datatakes where ICP could be found

In x-direction, 1 datatake (~0.2%) has an RMSE value above 30 m (1 GSD), whereas in y-direction, 5 datatakes (~0.8%) are above this threshold. For most of those datatakes, only very few GCP and ICP could be found during processing, making the results less reliable. The mean values are 13.71 m in x-direction and 8.08 m in y direction. This shows a very high geolocation accuracy for the datatakes where matching was possible. The requirement GRD-PCV-0155 is thus fulfilled.

The average boresight angles, which can be interpreted as the correction and thus the error of the scene if no GCPs could have been found, corresponds to approximately -18 m in x direction with a standard deviation of approximately 19 m and -31 m in y direction with a standard deviation of approximately 23 m on ground. It is reasonable to assume that the scenes where no GCPs could be found are in the same accuracy range and thus well within the requirement of 100 m (GRD-PCV-0150). Note that the x and y direction mentioned in this report are not in the image coordinate system but in UTM, as the evaluation is done on L1C products.

7.6.3.1 Geometric accuracy

EnMAP L1C products are matched against a reference image (Sentinel-2 data, if not stated otherwise) by using image matching techniques to assess the geometric accuracy. At the obtained checkpoints (CP), statistics are calculated to provide mean and RMSE values for each scene (see Figure 7-27). Note that the obtained accuracy in the analysis is always w.r.t. the reference image. This report covers EnMAP data from 01.10.2023 to 31.12.2023. A random sample of 246 L1C tiles was selected based on visual inspection of the catalogue quicklooks (e.g. to avoid cloudy images).

The requirement GRD-PCV-0155 shall be fulfilled:

The geolocation accuracy at nadir look direction of level 1C and 2A products shall be better than 1 GSD (1 sigma) in each direction with respect to reference images provided that reference images are available and sufficient similarity.

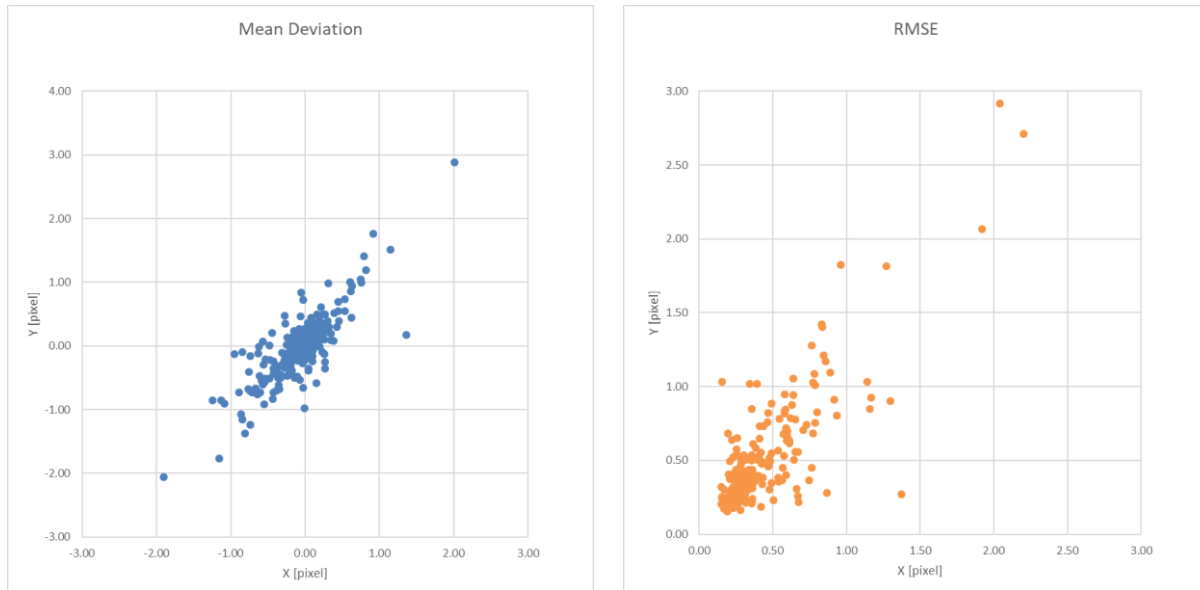


Figure 7-27 Mean deviation of EnMAP L1C products in pixel (left). RMSE value for EnMAP L1C products in pixel (right)

Note, that during processing the boresight angles and the geometric accuracy related quality flags are calculated on datatake level while in the figures and tables above, the accuracy is assessed per tile. The mean values over all 247 L1C tiles are -0.08 and -0.02 pixel in mean deviation with a standard deviation of 0.42 and 0.51 pixel while the mean RMSE values are 0.43 and 0.50 pixel, all in x and y direction respectively. The data show, that for the vast majority of scenes the accuracy wrt. reference image is better than one pixel and thus the requirements are fulfilled. Compared to the last geometric QC report, the values are very stable.

7.6.3.2 Co-registration accuracy

In this chapter, the co-registration accuracy is checked against the Space Segment requirement SRDS-PIM-0050 (EN-KT-RFW-003 is also to be considered here):

*The HS-Imager shall be designed such, that the geometric co-registration is $\leq 20\%$ of the nominal Ground Sampling Distance ($0.2 * GSD$ linear displacement in both directions).*

For the assessment of co-registration accuracy, the SWIR data of EnMAP L1C products are matched against the corresponding VNIR data and the mean deviation values shown in this section (Figure 7-28).

This report covers EnMAP data from 01.10.2023 to 31.12.2023. A random sample of 247 L1C tiles was selected based on visual inspection of the catalogue quicklooks (e.g. to avoid cloudy images).

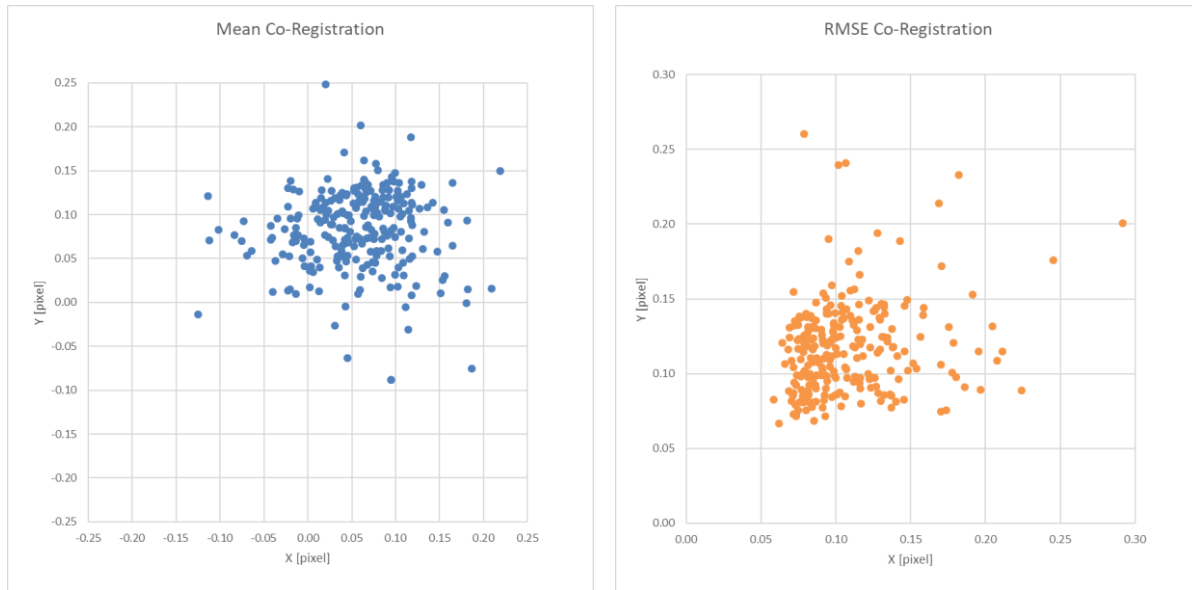


Figure 7-28 Mean deviation in pixel between VNIR and SWIR data of EnMAP L1C products (left). RMSE in pixel between VNIR and SWIR data of EnMAP L1C Products (right)

The data show, that the mean co-registration is in the order of 0.07 pixel both in x and y direction which is well within the requirement. Note that the theoretical accuracy of the used matching algorithm is 0.1 pixel, and as can be seen in the RMSE values, still some mismatches were not removed by the blunder detection techniques that were applied. The mean deviation over all analyzed tiles are 0.06 pixel in x-direction with a standard deviation of 0.06 pixel and 0.08 pixel in y direction with a standard deviation of 0.05 pixel. Compared to the results in the previous geometric QC report, the values are very stable.

7.6.3.3 Development of geometric performance

Since the launch of EnMAP on April 1st 2022, the geometric performance has been improved significantly. This was achieved by different geometric calibrations and processor updates. Table 7-25 shows the measures performed, their date and their effect.

Date	Measure	Effect
01.08.2022	Fix of attitude processing	Improvement of absolute geolocation (w/o matching)
20.09.2022	Boresight Calibration	Improvement of absolute geolocation (w/o matching)
03.11.2022	1 st Geometric Calibration	Improvement of absolute geolocation (w/o matching) Improvement of VNIR/SWIR co-registration (~0.8 pix -> ~0.4 pix)
11.02.2023	2 nd Geometric Calibration	Improvement of VNIR/SWIR co-registration (~0.4 pix -> ~0.15 pix)
29.03.2023	Processor update (v01.02.00)	Improvement of VNIR/SWIR co-registration (~0.15 pix -> ~0.06 pix)
05.05.2023	Processor update (v01.03.01)	Improvement of geolocation accuracy

Table 7-25 Improvement of geometric performance

Figure 7-29 shows the development of the co-registration accuracy, measured as described in previous section. Again, after a significant improvement since commissioning phase, over the last report periods the accuracy has been very stable.

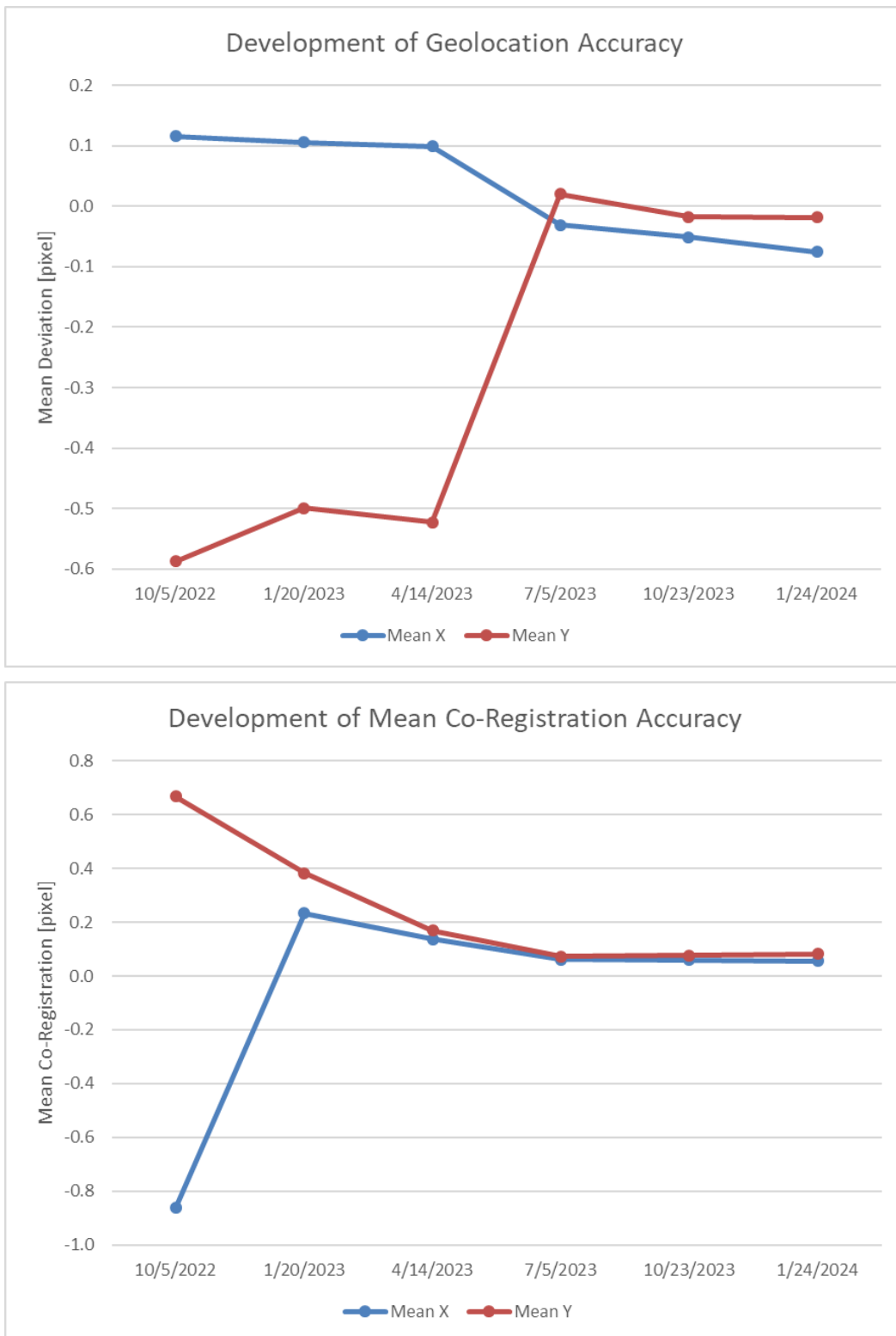


Figure 7-29 Development of co-registration accuracy based on the previous geometric QC reports

As most of the geometric processing – especially the matching against a reference image – is done on datatake level during L0 processing, the geometric accuracy and co-registration of data acquired earlier during the mission is not automatically improved when higher level products (L1B, L1C, L2A) are processed with the current processor version. However, during the currently ongoing L0 reprocessing of the whole



archive, the geometric processing is executed with the latest processor version and geometric calibration table to make sure that the best geometric quality and co-registration is reached also for the reprocessed data. Users can recognize reprocessed data by checking the metadata tag **archivedVersion**: if the version is 01.03.00 or higher, then the geometric performance should be as analyzed in this report.

7.6.4 Level 2A

7.6.4.1 Validity of generated L2A “water” data

7.6.4.1.1 Analyzed scenes

The following scenes were taken into consideration:

DataTake - ID	Tile - ID	Location	L2A Option	Cirrus / Haze Removal	Overall Quality
48472	2	Lake Elsinore	Water mode, water type “clear”	Cirrus	Nominal
48781	2	Lake Harsha	Water mode, water type “clear”	Cirrus	Nominal
49782	2	Lake Harsha	Water mode, water type “clear”	Cirrus	Nominal
48589	2	Lake Hume	Water mode, water type “clear”	Cirrus	Nominal
49784	2	Lake Hume	Water mode, water type “clear”	Cirrus	Nominal
48673	2	Lucinda	Water mode, water type “clear”	Cirrus	Reduced

The below listed parameters were checked for above mentioned scenes by EOMAP:

Parameter	Check
Masking (Land, Water, Clouds, etc.)	No issues found.
Adjacency correction	No issues found.
Retrieval of atmospheric properties	Issue found when setting different water types.
Cirrus – correction	No issues found.
Retrieval of water leaving reflectance	Issue found in context of signal-peaks in the blue spectral region.
Quality Mask	Issue found for the glint-quality - band

In the following the scene 48673, covering the area around Lucinda (Figure 7-30), is used to show some examples of the data checked here.

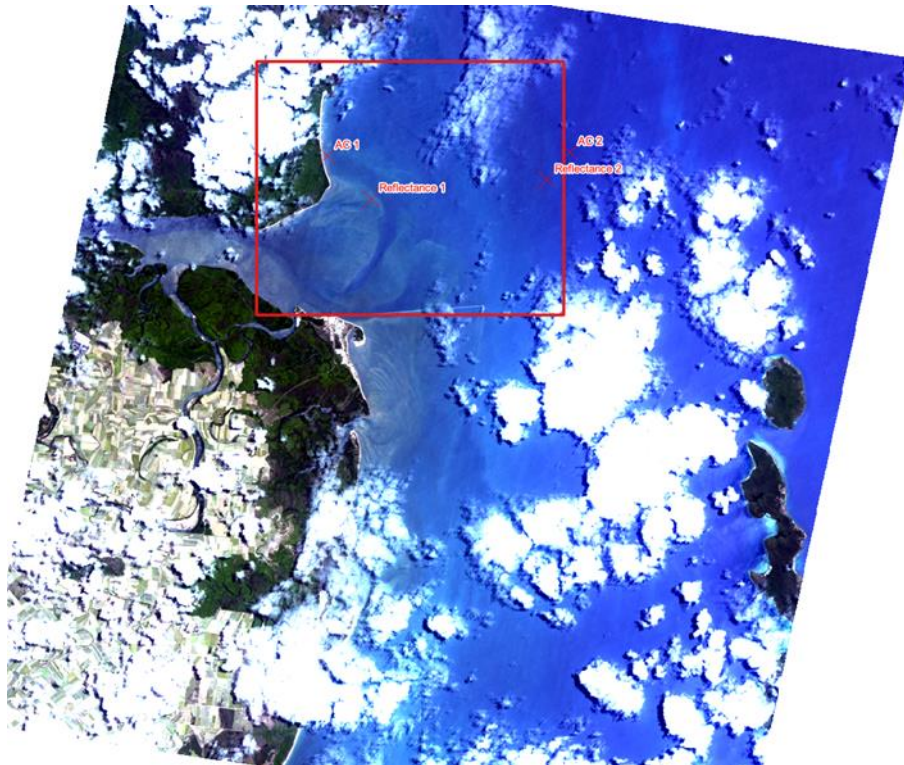


Figure 7-30 RGB - Quicklook of sceneID 48673; Red frame is the AOI for further investigation, the crosses show the sample – locations for the following analysis; Wavelengths for RGB: 611.02nm – 550.69nm – 463.73nm

7.6.4.1.2 Data Checks

- Masking

First, the water mask is checked. The water body and the clouds are correctly masked (see Figure 7-31).

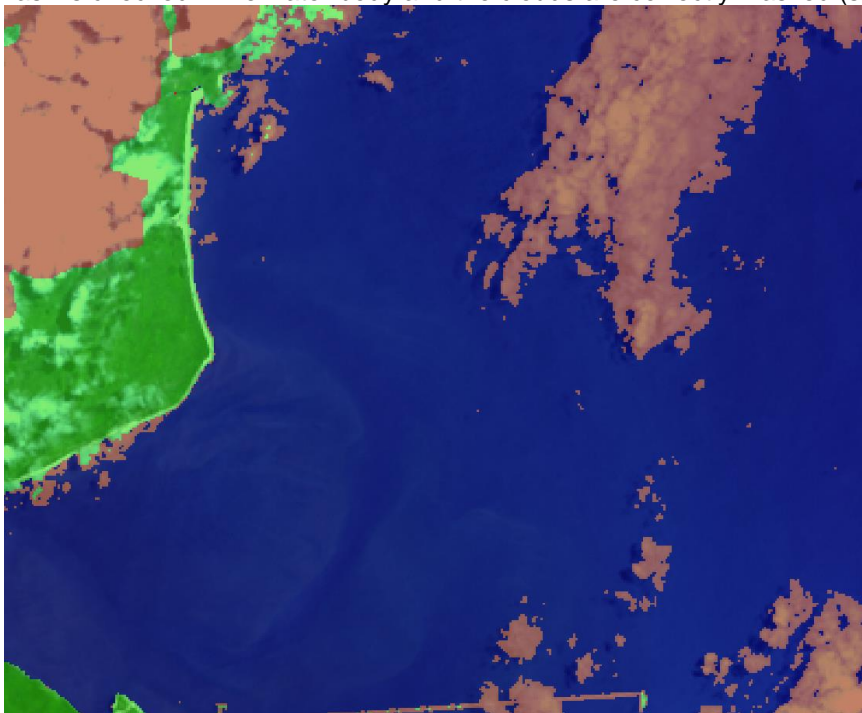


Figure 7-31 Masking within the AOI; Land in green, clouds in brown, water in blue

- Adjacency Correction

Next, we check for the adjacency correction using the two sites 'AC1' and 'AC2' showed in Figure 7-32.

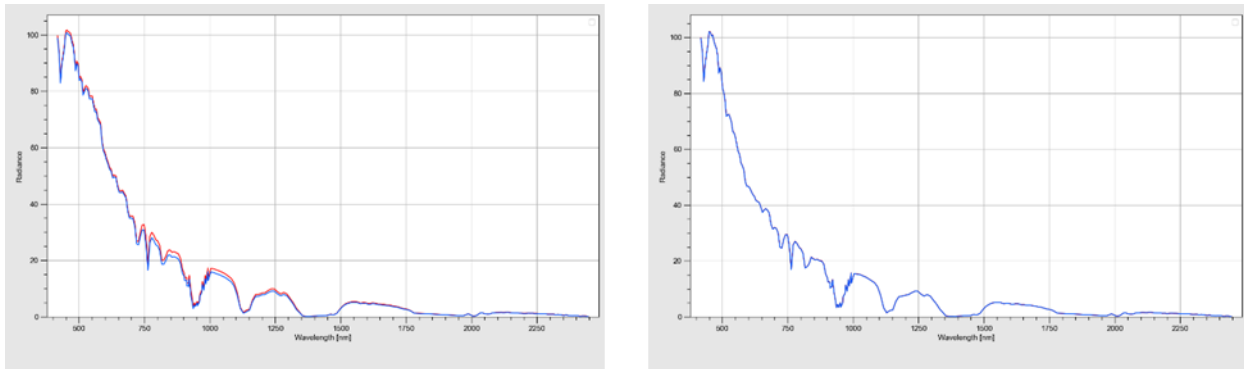


Figure 7-32 Red is the radiance without adjacency correction, blue corresponds to the spectrum after correction; Left: AC 1, Right: AC 2

In Figure 7-32, the influence of this correction on the spectrum is depicted. The adjacency effect is small, but noticeable in the sample-location AC1 (Left image in Figure 7-32) close to the shore. For the location offshore the correction has almost no effect, as the two lines are practically on top of each other, as one would expect. Summing up, the adjacency correction works as expected.

- Quality Mask

In Figure 7-33, the quality mask for the AOI within the scene is depicted. Note, that a grayscale was chosen, with a value range for 0 (bad quality) to 1 (high quality) reflecting the total quality of each pixel, where 0 corresponds to black and 1 to white. As shown, most of the water – areas were found to have a quality index of 0. In this scene, the high values of the aerosol optical thickness (AOT) derived from the atmospheric correction results in the low-quality values since such atmospheric conditions are difficult to correct. Overall, the atmospheric correction, as well as the quality assessment work as expected.

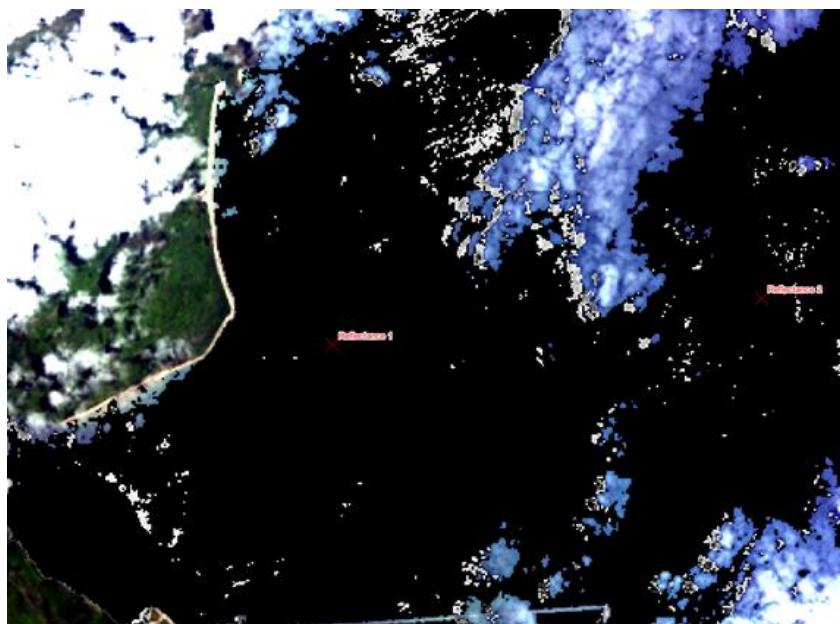


Figure 7-33 Quality mask for the AOI in grayscale of total quality

- Reflectance Product

To get a better impression of the product water leaving reflectance as the final one, Figure 7-34 shows the reflectance for the chosen AOI.

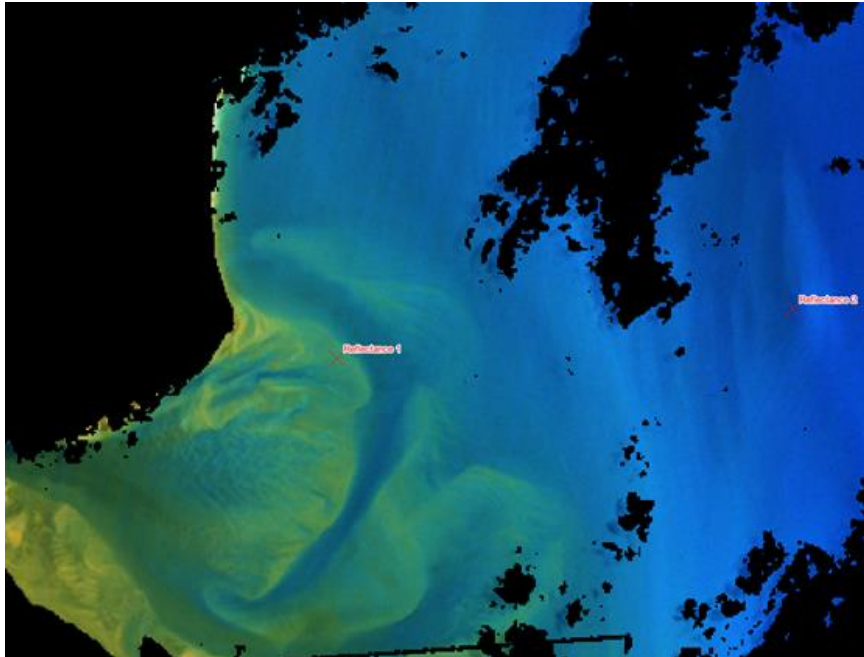


Figure 7-34 Water Leaving Reflectance for the AOI; Wavelengths for RGB: 611.02nm – 550.69nm – 463.73nm

For the two labeled locations, you can find the corresponding spectra in Figure 7-35.

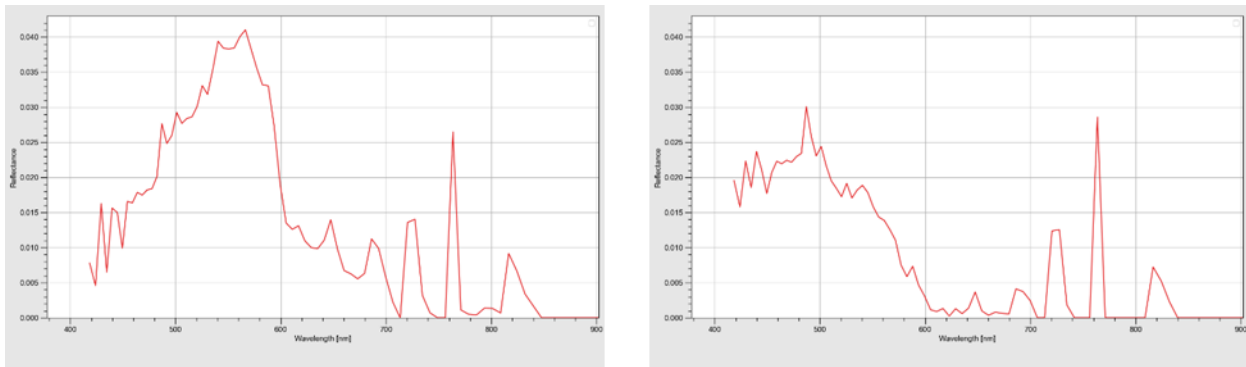


Figure 7-35 Water leaving reflectance for locations 'Reflectance 1' on the left and 'Reflectance 2' on the right

The left plot depicts a spectrum sampled from a point located in the - more turbid water area (location Reflectance 1 in Figure 7-35). The contribution of the turbidity can be seen in the spectral region around wavelengths from 535.42nm to 588.17nm. Also, there is still some signal in the infrared region reflecting the shallow water column. The right plot shows a curve characteristic for clear water (location Reflectance 2 in Figure 7-35). Both plots contain peaks for the wavelengths 429.46nm, 439.76nm, 487.09nm and 501.24nm that will be described further below. Contributions of the atmosphere can also be seen, for example for wavelengths 756.35nm and 816.61nm. The spikes present here are located in spectral regions where atmospheric absorption, mainly due to water vapor, plays an important role. In addition to the high AOT, which is detected and considered in the quality mask, this scene also seems to have a high fraction of water vapor. The atmospheric correction of the MIP processor dynamically corrects for the aerosols, but assumes a constant value for the water vapor, since aquatic applications typically focus on the visible range of the spectrum and discard spectral regions with high atmospheric absorption.

Overall, though the atmospheric conditions are challenging, the atmospheric correction, as well as the retrieval of the water leaving reflectance work as expected.

7.6.4.1.3 Details for the known issues

To fix the issues listed in the table above, the MIP-processor was already updated. This updated version is currently being integrated in the EnMAP-processor and will therefore be available in the next release.

The issues in context of water types and quality mask, respectively, are of technical nature and therefore not further described here. The spectral peaks were found to be related to the Fraunhofer lines of the solar spectrum which pinpoints to a problem of spectral resolution in these regions where the solar spectrum varies strongly. In the new processor version, the band width of the EnMAP bands are sampled at a higher spectral resolution, greatly diminishing the appearance of those peaks.

7.6.4.1.4 User Questions on the adjacency correction

Since some users raised questions about the effect of the adjacency correction, the following is intended to clarify those. For more details, we refer to https://www.enmap.org/data/doc/EN-PCV-TN-6008_Level_2A_Processor_Atmospheric_Correction_Water.pdf.

In the adjacency correction, the light that is reflected from a nearby bright land surface, scattered in the atmosphere, and thus increases the apparent radiance over water bodies is subtracted from the measured radiances. In principle, the activation of the adjacency correction would lead to smaller radiances and thus to smaller water reflectance. However, there is another correction step that takes place between adjacency correction and the calculation of the water reflectance, namely atmospheric correction. Depending on the spectral characteristics of the nearby land surface which contributes to the adjacency effect and on the atmospheric conditions, it can happen that in the absence of adjacency correction, the atmospheric correction overcompensates the missing adjacency correction and results in lower water reflectance values than with adjacency correction. We would like to stress that even though the nonlinear interplay of the correction steps is not easily predicted, stable results for a wide range of atmospheric conditions can only be obtained when both physical effects are accounted for.

7.6.4.2 Validity of generated L2A “land” data

7.6.4.2.1 Analyzed scenes

Within the time interval between 2023-10-01 and 2023-12-31, an interactive in-depth analysis has been conducted for the following scenes:

dataakeID	tileID	date	location	L2A option	cirrus and haze removal	overall Quality	processor version
44414	33	03.10.2023	Paznauntal, Alpes	Land	Cirrus	V010401	Nominal
47045	32	11.10.2023	Mittenwald, Alpes	Land	No	V010401	Nominal
50937	7	13.11.2023	Antarctica	Water	No	V010401	Nominal
52868	9	28.11.2023	Lake Chad, Chad	Combined	No	V010401	Nominal
54867	3	19.12.2023	Pinnacles, Australia	Land	No	V010401	Nominal
55046	1	20.12.2023	Puebla, Mexico	Land	No	V010401	Nominal
55956	2	22.12.2023	Conakry, Guinea	Combined	No	V010401	Nominal

Table 7-26 Datatake ID of analyzed land products

For the selection of L2a data, care was taken to ensure a high degree of variety with respect to the geographical location of the data, external conditions (cloud cover) during the data take and processing parameters.

7.6.4.2.2 Data Checks

- Checking water masks in areas with steep slopes (DT 44414 and DT 47045) (see ticket #444)

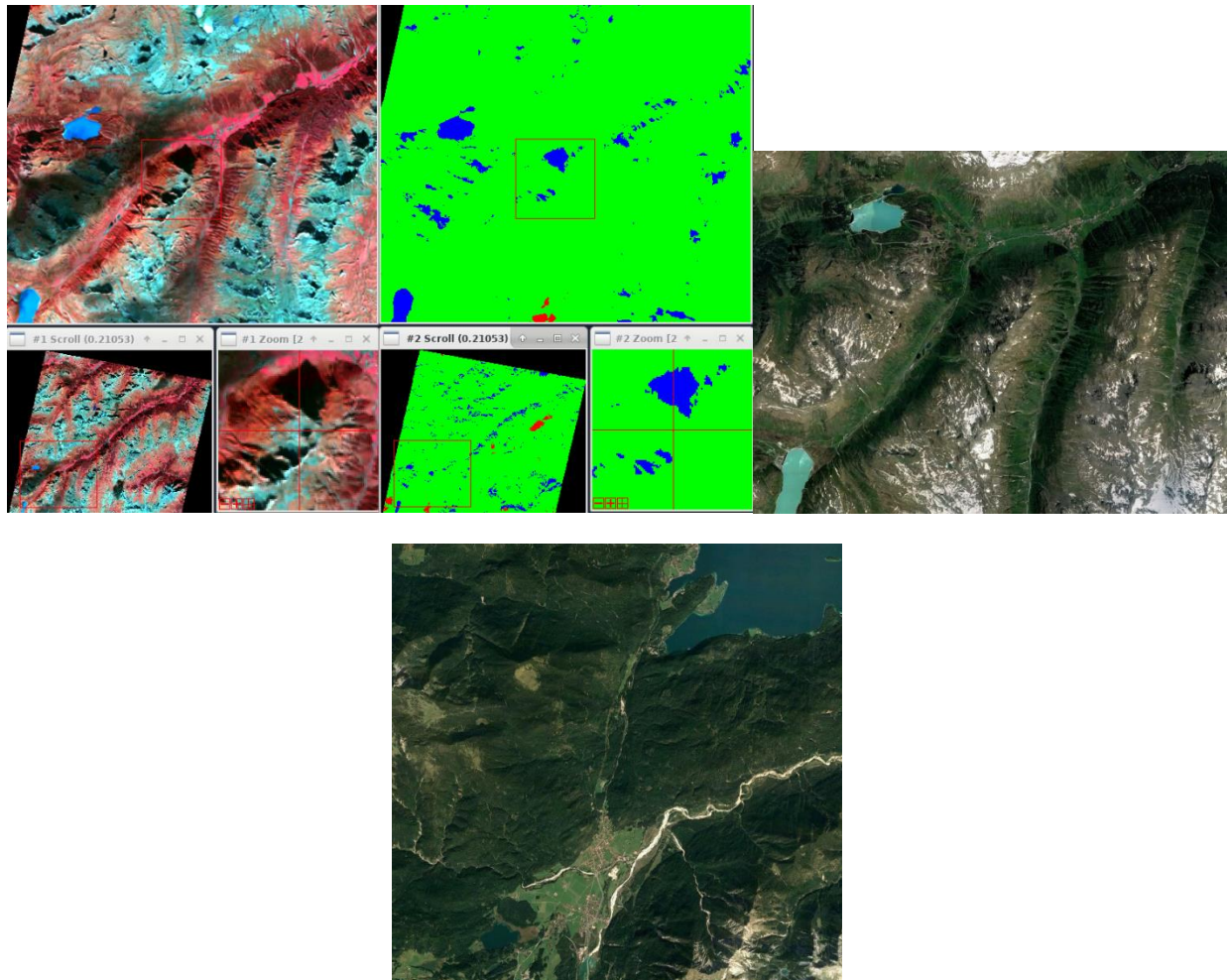


Figure 7-36 From left to right: EnMAP L2A CIR, quality classes, Google Earth

Dark vegetation areas on steep shaded slopes are classified as water (Figure 7-36) although all pixels with slope > 7 degrees are excluded from the water classification. Further investigation is needed.

- Checking water masks (DT 52868)

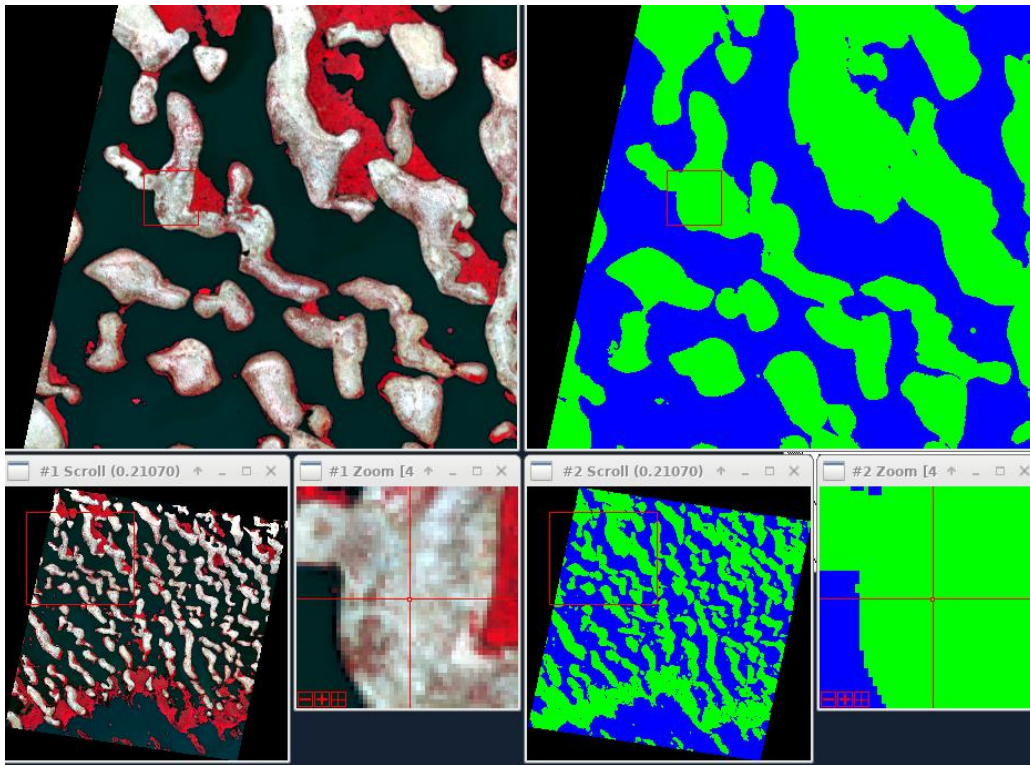


Figure 7-37 Left: EnMAP L2A, Right: QL classes (blue = water, green = land)

Water mask in the given scene displaying Lake Chad does not show any inconsistencies. Water and land are detected correctly. Results as expected.

- Checking cloud masks (DT 47045)

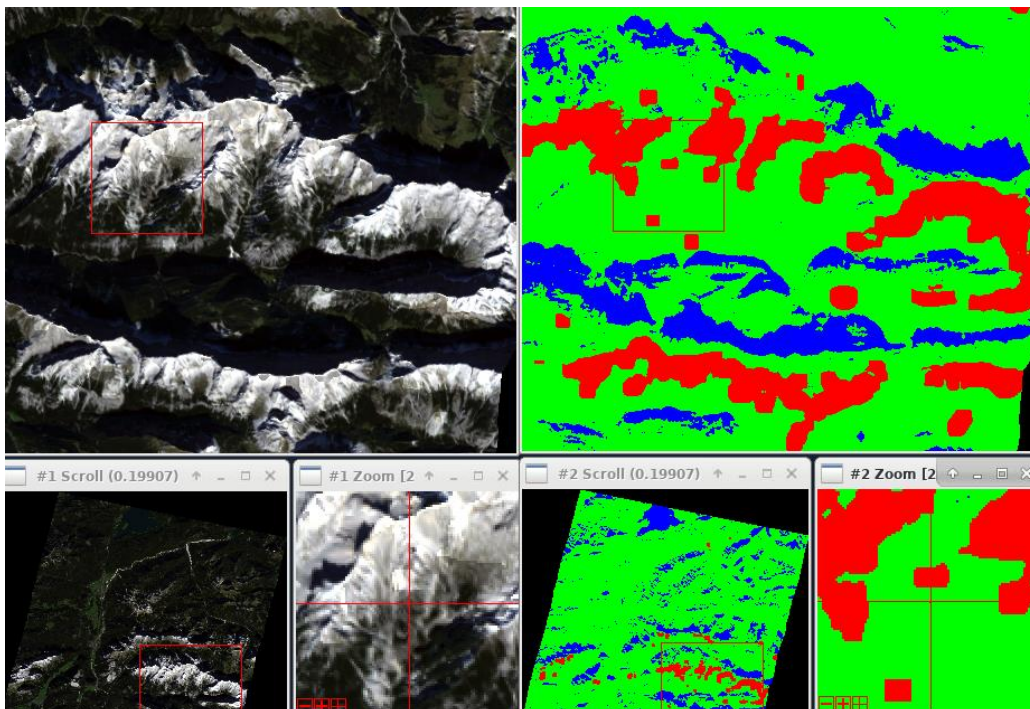


Figure 7-38 From left to right: EnMAP L2A RGB, quality classes (red = cloud)

Bright rocks are masked as clouds in the mountains (Figure 7-38). This is due to their spectral similarity. Further adaptation for better differentiation can be considered.

- Checking haze masks (DT 52868)

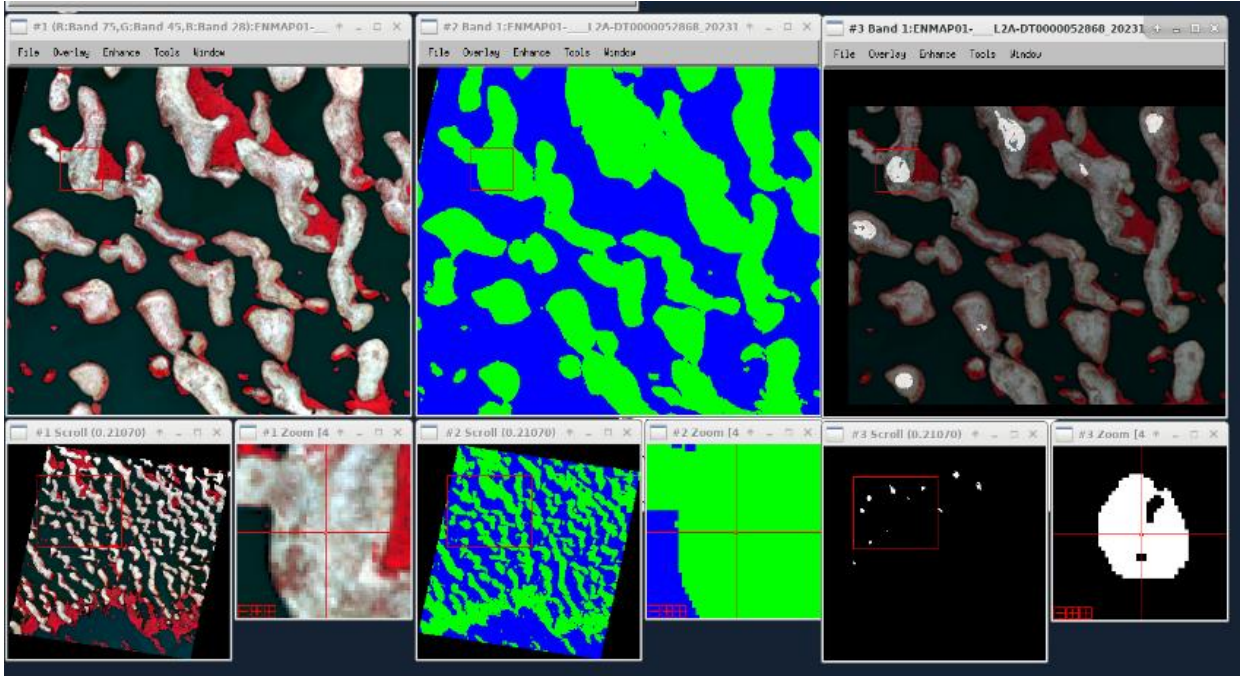


Figure 7-39 Left: EnMAP L2A, : Middle: QL classes (blue = water, green = land); Right: EnMAP L2A overlaid by haze mask
There are a few areas (only over land) labeled as hazy areas.

- Checking haze mask in areas with occurring fires (DT 55956)

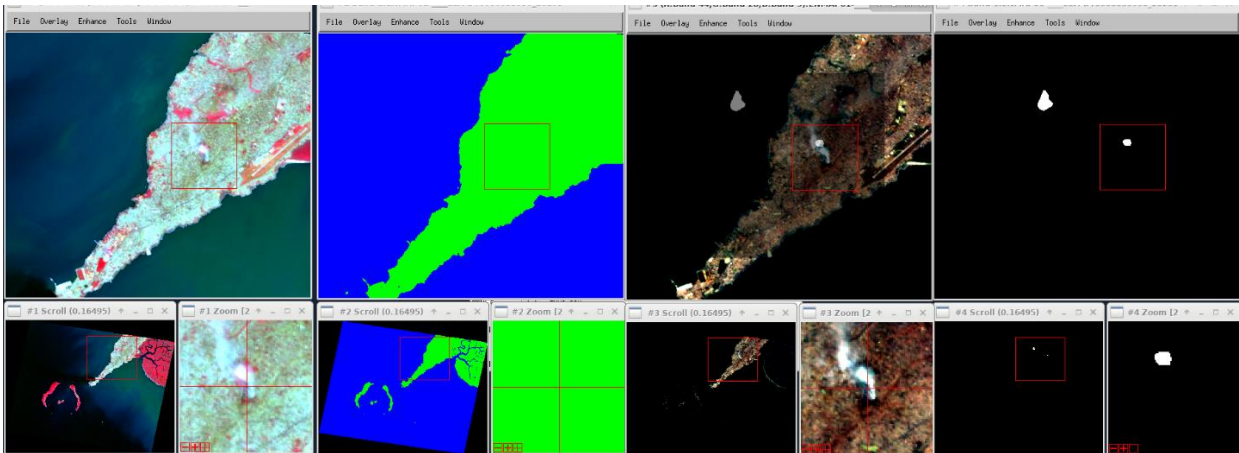


Figure 7-40 From Left: EnMAP L2A (CIR); QL classes (blue = water, green = land); EnMAP L2A (RGB) overlaid by haze mask; Haze mask

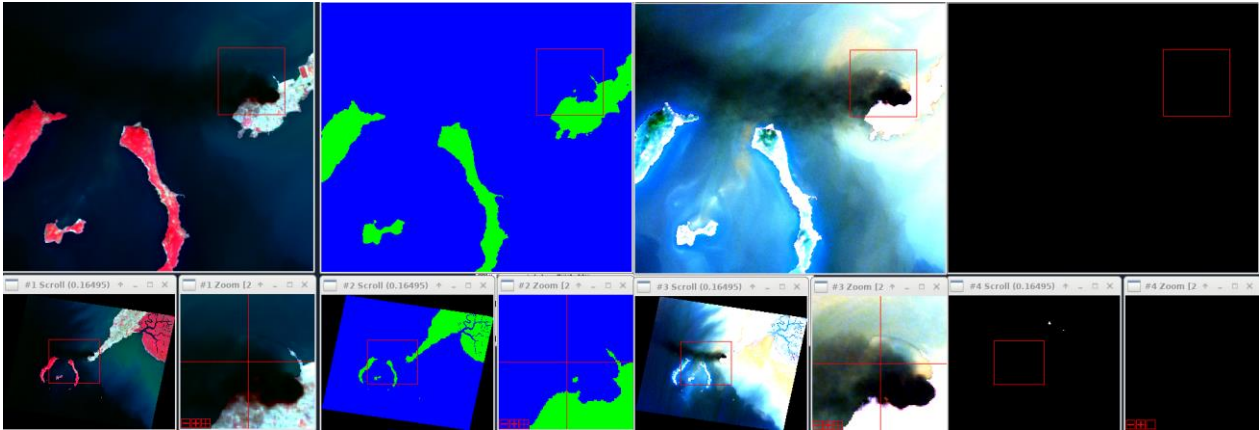


Figure 7-41 From Left: EnMAP L2A (CIR); QL classes (blue = water, green = land); EnMAP L2A (RGB), image stretched; Haze mask

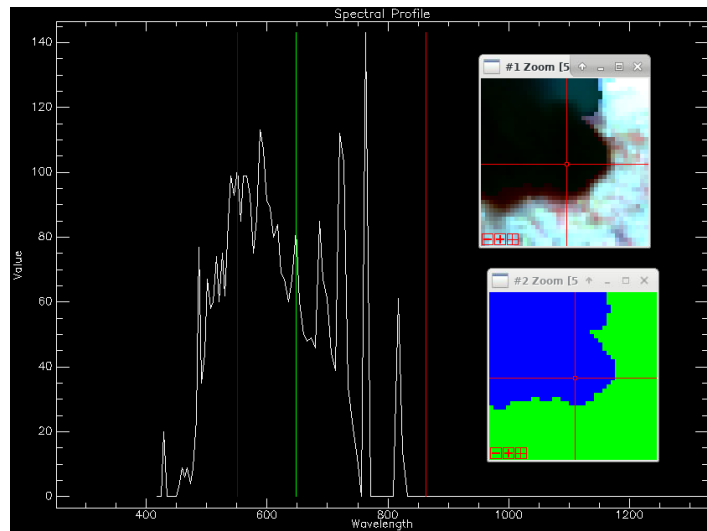


Figure 7-42 Reflectance of smoke plume displaying the position of the corresponding pixel in the scene (EnMAP L2A and QL classes)

DT 55956 displays an oil depot explosion in Conakry. The smoke plume was not detected as haze (Figure 7-41). This is due to the fact, that the plume is very dark, and is therefore classified as water. The only haze detected within the scene is shown in Figure 7-40, which is correctly referring to smoke.

- Checking land/water and snow mask (DT 54867)

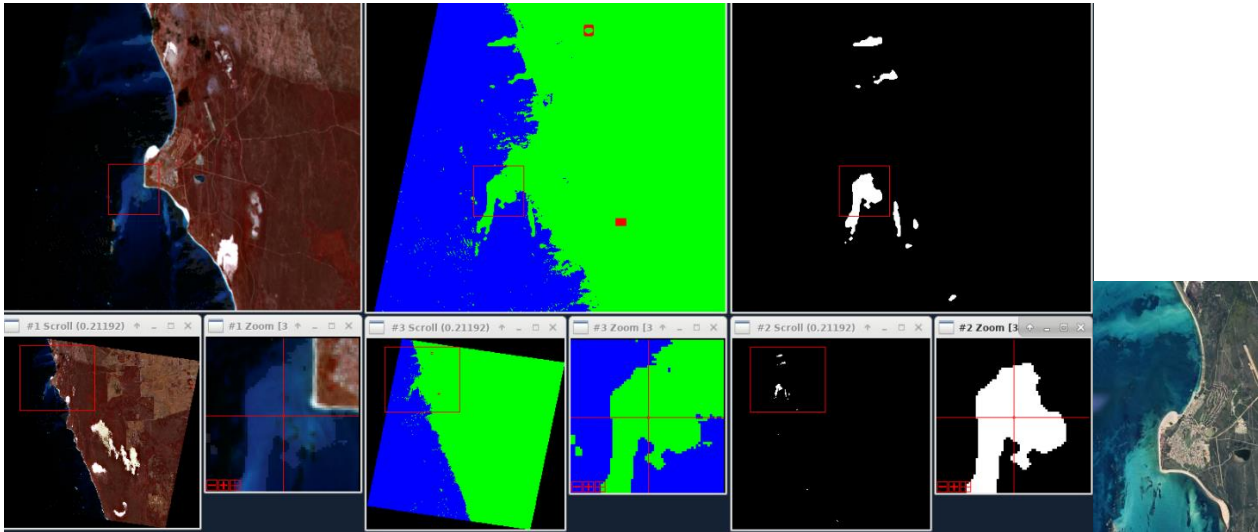


Figure 7-43 From Left: EnMAP L2A (CIR); QL classes (blue = water, green = land); Snow mask, Google Earth

Areas at the coastal line / shallow water (coral reef?) misclassified as land, and thus these areas were classified as snow. This issue is currently being further investigated.

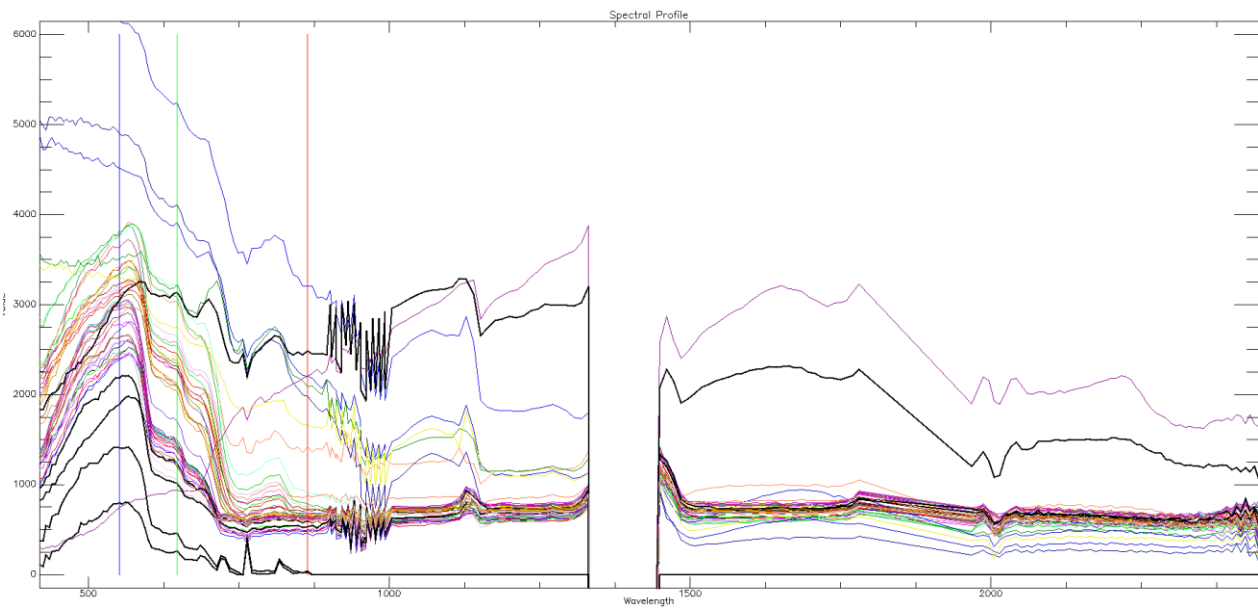


Figure 7-44 Spectra collected within the areas classified as snow (colored) and outside (black)

8 External Product Validation

During the reporting period, external data product quality monitoring activities checked all standard quality parameters. EnMAP products from the latest processor and archiving versions were validated. Some in-situ matchups not integrated in the last quarter were completed, and new ones were created. Images acquired after the brief outages (13.-27. October and 07.-19. December 2023) were carefully examined into the validation.

8.1.1 Level 1B

The following validation scenarios were used to validate about 200 Level 1B products in the reporting period:

- TOA Radiance
- Spatially coherent radiometric miscalibration (striping artifacts; along- and across-track)
- Signal-to-Noise Ratio (SNR)
- Keystone
- Cross-matchups with EnMAP, EMIT, and PRISMA

The latest TOA Radiance comparisons based on earth data takes, created in the reporting period, are not yet available at the end of the reporting period. However, some matchups from the previous quarter were included in the validation statistic. The general trend of the radiometric miscalibration was verified, and the consolidated uncertainty statistic still meets the mission requirements of < 5% radiometric miscalibration and shows no significant changes.

No significant anomalies were detected regarding the VNIR and SWIR across-track direction spatially coherent radiometric miscalibration. Slight residual low-frequent across-track undulations are still inherent to the data cubes, which will be fixed after an update of the VNIR gain matching. Also, SWIR along-track artifacts at wavelengths with a vital gradient/feature are still detectable but will be compensated after a processor update at the beginning of the next quarter. All mentioned artifacts are well within the mission requirements of < 5 %.

The SNR assessment was updated based on 163 reprocessed tiles and was found to be very stable compared to the previous evaluations and still inside the mission requirements.

For the VNIR and SWIR Keystones, also no significant changes were detected.

Initial results for the cross-validation between PRISMA, EMIT, and EnMAP indicate a good TOA reflectance fit between the missions within <10% TOA reflectance. Further investigations and additional matchups will bring more insight into this relative evaluation of EnMAP compared to the other systems.

8.1.2 Level 1C

The following Level 1C validation scenarios have been performed:

- VNIR-to-SWIR spatial co-registration
- Absolute spatial accuracy

The spatial co-registration between VNIR-to-SWIR for products with an archived version $\geq 01.04.00$, an RMSE of 3.4 m in X and 3.8 m in Y direction is achieved. Thus, the geometric co-registration has reached a stable level, well inside the mission requirements of < 30 % of a pixel.

Significant improvements have been recognized for the absolute spatial accuracy validation. With an RMSE of 10.2 m in X and 12.6 m in Y for tiles with an archived version $\geq 01.04.00$, the achieved absolute spatial accuracy is well inside the mission requirements (<30m with GCPs in the image, <100 m without GCPs).

8.1.3 **Level 2A**

Several in-situ matchups, generated during the last quarter and newly generated, were added to the L2A land and water quality assessment.

Land

The additional matchups stabilized the RMSE, accuracy, and precision assessment, confirming the overall tendency and pattern. At the beginning (<500 nm) and ending (>2250 nm) of the wavelength domain, slightly higher residuals (<3% RMSE, accuracy, and precision) can be identified. The majority is around 2 % for the rest of the wavelength domain. All measures are generally well inside the mission requirements for BOA reflectance of 5%.

Water

Several L2A normalized water leaving matchups were integrated into the statistic assessment during the reporting period, indicating that all valid matchups meet the mission requirements.

The EnMAP normalized water reflectance products (for preprocessing versions $\geq 01.04.00$) over various water sites show values within the mission requirements. Slightly higher residuals between 450-550 nm have been identified, which can be traced back to not distinguishing between clear, turbid, and high turbid waters in the atmospheric correction. All images are processed for the same optical water type (see section 7.4)."

8.1.4 **Summary of External Product Monitoring**

We did all the essential validation scenarios and checks during the reporting period using the latest EnMAP preprocessing and archived versions. Every validation is nominal regarding their respective mission requirements and the geometric performance regarding absolute spatial accuracy, significantly improved for products with an archived version $\geq 01.04.00$.

9 Others

EnMAP Publications:

EnMAP Presentations:

- A. Schickling, "EnMAP: The German Hyperspectral Mission", Presentation at the 1st EnMAP User Workshop. October 10-11, 2023. Online Workshop.
- S. Chabrillat and the EnMAP Science Team, "Scientific exploitation preparation and support of the EnMAP satellite mission: Update and current activities". Presentation at the 1st EnMAP User Workshop. October 10-11, 2023. Online Workshop.
- E. Carmona, S. Engelbrecht, M. Habermeyer, H. Mühle, M. Pato, K. Wirth, "The Ground Segment of the EnMAP mission: from tasking to product download". Presentation at the 1st EnMAP User Workshop. October 10-11, 2023. Online Workshop.
- N. Pinnel, A. Schickling, L. La Porta, S. Chabrillat, S. Foerster, C. Lenzen, H. Mühle, E. Carmona, S. Fischer, "The EnMAP User Inquiries and Ground Segment Operation Activities". Presentation at the 1st EnMAP User Workshop. October 10-11, 2023. Online Workshop.
- P. Schwind, M. Pato, M. Schneider, R. de los Reyes, M. Langheinrich, M. Bachmann, B. Gerasch, "The EnMAP processing chain". Presentation at the 1st EnMAP User Workshop. October 10-11, 2023. Online Workshop.
- D. Marshall Ingram, M. Pato, E. Carmona and R. de los Reyes, "EnMAP Spectral and Radiometric Calibration". Presentation at the 1st EnMAP User Workshop. October 10-11, 2023. Online Workshop.
- M. Langheinrich, R. de los Reyes, M. Bachmann, "The EnMAP Ground-Segment L2A Processor - Products and Specifics". Presentation at the 1st EnMAP User Workshop. October 10-11, 2023. Online Workshop.
- M. Bachmann, M. Schneider, B. Gerasch, S. Holzwarth, M. Habermeyer, M. Pato, E. Carmona, "Operational data quality control and instrument monitoring for the spectral, radiometric and geometric data properties within the EnMAP Ground Segment". Presentation at the 1st EnMAP User Workshop. October 10-11, 2023. Online Workshop.
- M. Brell, L. Guanter, D. Scheffler, K. Segl, N. Bohn, S. Chabrillat, S. Foerster, M. Soppa, A. Bracher, M. Bachmann, R. Kokaly, C. Ong, J. Moreno, F. Gascon, R. O. Green, E. Carmona, M. Pato, A. Schickling, S. Fischer and the EnMAP validation team, "EnMAP external validation from the EnSAG/EnMAP science segment". Presentation at the 1st EnMAP User Workshop. October 10-11, 2023. Online Workshop.
- E. Carmona, M. Habermeyer, H. Mühle, M. Pato and N. Pinnel, "The EnMAP Ground Segment User Services and Products". Poster presentation at 12th Workshop on Hyperspectral Image and Signal Processing: Evolution in Remote Sensing, Oct. 31 – Nov. 02, 2023. Athens, Greece.
- M. Langheinrich, R. de Los Reyes, "The ENMAP L2A Water Processor: Operational Performance and Application of ENMAP Dedicated Water Reflectance Products". Oral presentation at 12th Workshop on Hyperspectral Image and Signal Processing: Evolution in Remote Sensing, Oct. 31 – Nov. 02, 2023. Athens, Greece.
- N. Pinnel. "Environmental Mapping and Analysis program – The EnMAP Mission", Invited Lecture at Albert-Ludwigs-Universität, Freiburg, 07.12.2023.
- N. Pinnel. „EnMAP der fliegende Umweltdetektiv“, Special Exhibition at Deutsches Museum, 19.12.2023